

Journal Pre-proofs

NiCo₂O₄ nanorod: Synthesis and electrochemical sensing of carcinogenic hydrazine

Velayutham Sudha, Sakkarapalayam Murugesan Senthil Kumar, Rangasamy Thangamuthu

PII: S1387-7003(20)30101-5
DOI: <https://doi.org/10.1016/j.inoche.2020.107927>
Reference: INOCHE 107927

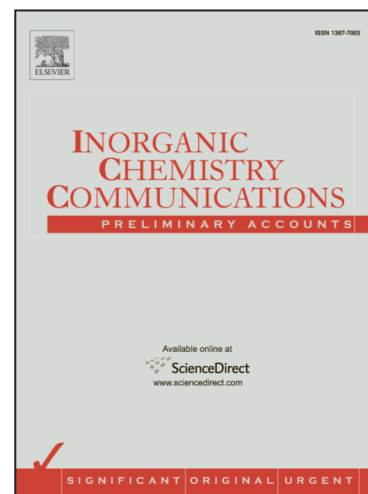
To appear in: *Inorganic Chemistry Communications*

Received Date: 23 January 2020
Revised Date: 20 March 2020
Accepted Date: 2 April 2020

Please cite this article as: V. Sudha, S. Murugesan Senthil Kumar, R. Thangamuthu, NiCo₂O₄ nanorod: Synthesis and electrochemical sensing of carcinogenic hydrazine, *Inorganic Chemistry Communications* (2020), doi: <https://doi.org/10.1016/j.inoche.2020.107927>

This is a PDF file of an article that has undergone enhancements after acceptance, such as the addition of a cover page and metadata, and formatting for readability, but it is not yet the definitive version of record. This version will undergo additional copyediting, typesetting and review before it is published in its final form, but we are providing this version to give early visibility of the article. Please note that, during the production process, errors may be discovered which could affect the content, and all legal disclaimers that apply to the journal pertain.

© 2020 Elsevier B.V. All rights reserved.



NiCo₂O₄ Nanorod: Synthesis and Electrochemical Sensing of Carcinogenic Hydrazine

Velayutham Sudha ^{a,b}, Sakkarapalayam Murugesan Senthil Kumar ^{a,b}, Rangasamy Thangamuthu ^{a, b*}

^a Materials Electrochemistry Division (MED), CSIR-Central Electrochemical Research Institute (CSIR-CECRI), Karaikudi-630 003, Tamil Nadu, India.

^b Academy of Scientific and Innovative Research (AcSIR), CSIR-Central Electrochemical Research Institute, Karaikudi- 630 003, Tamil Nadu, India.

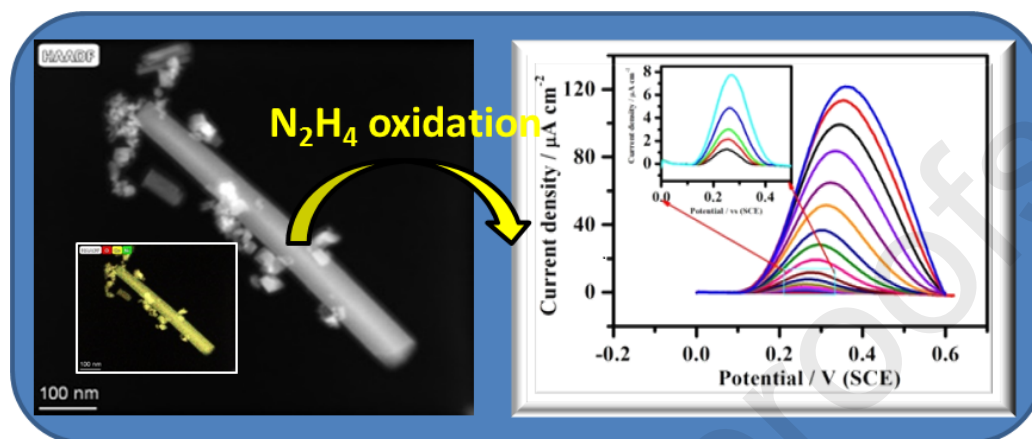
* To whom correspondence should be addressed. E-mail: thangamuthu@cecri.res.in; thangamuthu_r@yahoo.co.uk; Phone: +91-04565-241-350.

Abstract

In this work, we explored a simple hydrothermal process to tune the NiCo₂O₄ morphology into well defined rod structure with nanoparticle on it. The as prepared NiCo₂O₄ was characterized by various characterization studies such as XRD, Raman, FT-IR, TGA and HRTEM. The electrochemical sensing of hydrazine on NiCo₂O₄ nanorod was examined by cyclic voltammetry and differential pulse voltammetry techniques. The NiCo₂O₄ shows excellent electrocatalytic performance for the anodic oxidation of hydrazine. Interestingly, NiCo₂O₄ retain considerable current response after 50 cycles at 25 mV s⁻¹. The Ni and Co in bimetal oxides enhanced the current response due to their electroactive sites. The developed NiCo₂O₄ not only enhanced the current response of hydrazine but also exhibits good stability. NiCo₂O₄ demonstrates excellent detection limit and sensitivity of 260 nM and 48.25 $\mu\text{A cm}^{-2}$

mM⁻¹, respectively. For practical application, NiCo₂O₄/GCE was used for the sensing of hydrazine in real water samples.

Key words: Hydrazine, NiCo₂O₄, Hydrothermal method, Electrochemical sensing.



Scheme 1. Schematic illustration of NiCo₂O₄ characterization and electrochemical sensing of hydrazine.

1. Introduction

Hydrazine is widely used in fuel cell, food production, pharmaceutical intermediates, rocket fuel, pesticides production, blowing agent, dye industries, oxygen scavengers and so on [1–5]. The Environmental Protection Agency (EPA) identified hydrazine as a poisonous chemical and the proposed level in the commercial effluents is 1 ppm. Due to volatile nature of hydrazine, it is easily adsorbed on the human skin and damage the living organism especially, liver, blood production system and kidney [6]. Vernot et al., found that exposure to hydrazine for long time causes inhalation problem in different animals. Rats, hamsters, mice and dog were analysed post exposure of 18 months, 1 year, 15 months, 38 months, respectively. Male and female rats disclose dose-dependent prevalence of well-disposed nasal adenomatous polyps and smaller numbers of malignant nasal epithelial tumours after 1 year of exposure to hydrazine and 18 months post exposure holding [7], DNA damage [8] and

irreversible deterioration of nervous system [9]. Due to large consumption in industrial use, hydrazine and derivatives are commonly detected in atmosphere and it creates health hazardous particularly, in human. Nowadays, numerous methods are available to extensively detect the concentration of hydrazine including spectrophotometry [9], potentiometry [8], chemiluminescence [10], fluorimetry [11], gas chromatography-mass spectrometry [12], coulometry [13] and electrochemical method [14]. Compared with other method, electrochemical technique possesses many advantages including high sensitivity, portable, cost effective and simple operating procedure. Additionally, electrochemical method is a good modest substitute for the detection of hydrazine. Bare electrode suffers the disadvantages of high over potential and low sensing ability (signals) [15]. Commonly, the electrode surface was modified with nanostructured metal oxides, bimetal oxides, material possessing high surface area, catalytic activity and conductivity which improve the sensing signals of the analytes. Metal oxides are one of the investigated nanomaterials in the case of biotic and industrial applications due to their redox properties and catalytic activity. Mixed MOs are single phase bi-MOs consist of nickel and cobalt cations which have excellent electrocatalytic activity due to its synergetic effect in the case of mixed valence state and complex chemical composition either than the combination of nickel oxide and cobalt oxide [16]. The spinel NiCo_2O_4 is a transition metal oxide which has high theoretical capacity, excellent electrical conductivity, easy preparation procedure, easily controllable morphologies and environmental friendly. NiCo_2O_4 adopts the pure spinel form in their all the nickel (Ni) ions occupies octahedral (Oh) site and Co ions occupy both tetrahedral (Td) and Oh sites [17,18].

Recently, researchers reported that the NiCo_2O_4 modified electrode were used for the sensing of various bioanalytes and environmental pollutants such as ascorbic acid, uric acid, dopamine, glucose, lead and cadmium [19–21]. Due to their good electronic conductivity in

the form of mixed valences of Ni and Co cations is a beneficial for the fast electron transfer and it has excellent redox activity than to NiO and Co₃O₄ [16,22,23]. For the reason that, NiCo₂O₄ has atleast two order of higher magnitude than nickel oxide and cobalt oxide hence, it possess potential applications in the field of lithium ion batteries, supercapacitor, electrocatalyst optoelectronic devices and electrochemical sensor [24–30]. Prathap et al., already reported that NiCo₂O₄ was used for the detection of lindane which provides excellent sensing ability than single component oxides [30]. Recently, many methods are there for the preparation of NiCo₂O₄ nanomaterials with several structures which include nanoparticles, nanowire, nanoneedle, nanosheet, nanoflake and nanoflower [31–36]. The spinel oxides which has cobalt such as CuCo₂O₄, MnCo₂O₄, NiCo₂O₄, ZnCo₂O₄, MgCo₂O₄, etc. exhibit great attention due to their physicochemical properties, technological applications, sensors to electrode materials, catalysts and electrochemical devices [37]. In the present work, a hydrazine sensor was successfully developed using NiCo₂O₄ broken nanorod as nanoparticle were situated on NR. NiCo₂O₄ NR/GCE shows pronounced performance for the detection of hydrazine in terms of sensitivity, selectivity, reproducibility and stability. There are no reports available for the detection of hydrazine using NiCo₂O₄ NR modified electrode.

2. Experimental section

2.1. Materials

CoCl₂.6H₂O, NiCl₂.6H₂O, urea were purchased from Merck. Disodium hydrogen phosphate (Na₂HPO₄) and monosodium hydrogen phosphate (NaH₂PO₄) purchased from Sigma Aldrich. These chemicals were used to prepare the phosphate buffer supporting electrolyte solution (PBS) throughout the electrochemical measurements. All the chemicals were used directly without any other purification. Throughout the study, Milli-Q water with a resistivity of 18.2 MΩ collected from Mill-Q instrument. The collected Milli-Q water was used for the experimental solution preparations.

2.2. Synthesis of nanostructured NiCo₂O₄

NiCo₂O₄ was prepared by hydrothermal method. Initially, 1 g of CoCl₂.6H₂O and 0.5 g of NiCl₂.6H₂O and 1 g of urea were dissolved in 30 mL of deionized (DI) water and stirred continuously until pink colour was observed. The transparent pink solution was transferred to the Teflon lined stainless autoclave. The sample was heated at 130 °C for 6 hrs. Then, the solution was cool down to room temperature followed by washing with DI water and ethanol for more than five times. The sample was dried in vacuum over at 80 °C for 6 hrs. To end, the powdered sample was calcined 400 °C under air atmosphere at a heating rate of 5 °C/min for 3 hrs. The absolute products were examined and used for electrochemical studies. Similar procedure was followed for the synthesis of NiO and Co₃O₄.

2.3. Characterizations

The sample phase purity of the NiCo₂O₄ material was examined by X-ray diffraction (XRD) studies by Cu K α radiation ($\lambda = 0.15$ nm using Bruker D8 ADVANCE X-ray diffractometer within the range of 10 – 80°. Thermogravimetric analysis (TGA), by TGA/DTA system (Model of SDT Q600), was performed to explore the material decomposition temperature in the heating range of 0 °C to 590 °C in an open airspace. Fourier transform infra-red (FT-IR) spectroscopy for powder sample was accomplished by KBr pellet method using Bruker Optik GmbH, Germany Model No: TENSOR 27 in the scale from 400 to 4000 cm⁻¹. Raman spectroscopic study was examined by He–Ne laser (wavelength $\lambda = 633$ nm) using RENISHAW I laser Raman microscope in order to understand the chemical behaviour of the material. The chemical composition (EDAX) of the prepared samples was characterized by scanning electron microscope using TESCAN (Supra 55VP) operating at an accelerating voltage of 30 kV. NiCo₂O₄ was studied by Field emission scanning electron microscopy (FESEM) (Oxford instrument). The structural features were

studied by transmission electron microscopy (TEM; JEOL-JEM 2010 and TecnaiTM G² F20, FEI which operate with an accelerating voltage of 200 kV) The structural features of the material were observed using high resolution transmission electron microscopy (HRTEM; TecnaiTM G² TF20 working at an accelerating voltage of 200 kV). Elemental compositions and survey scan of the prepared NiCo₂O₄ material was probed using Mg K α (1253.6 eV) as X-ray source (Thermo Scientific, MULTILAB 2000) via X-ray photoelectron spectroscopy (XPS) using Theta Probe AR-XPS system.

2.4. Electrochemical measurement

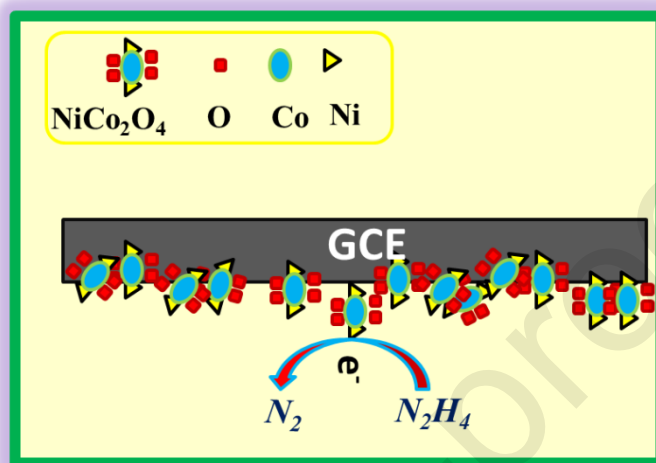
The **hydrazine** sensing performance of NiCo₂O₄ was studied using differential pulse voltammetry (DPV) and cyclic voltammetry (CV) techniques by AUTOLAB PGSTAT302N using three electrodes system with cleaned glassy carbon electrode (GCE; 3 mm diameter electrode geometric area=0.07 cm²) as working electrode, platinum electrode as counter electrode and Hg/HgCl₂/KCl_(sat) (saturated calomel electrode (SCE)) was used as reference electrode. Highly-pure N₂ gas used to purge into the experimental suspension before initiation of each experiments in order to remove the dissolved O₂ in the PBS (0.1 M, pH = 7). The electrocatalytic behaviour of **NiCo₂O₄ NR/GCE** towards oxidation of **hydrazine** was examined at room temperature.

2.5. Preparation of NiCo₂O₄ NR/GCE

Prior to the modification, bare GCE was polished with alumina slurry subsequently rinsed thoroughly in Mill-Q water and ultra-sonicate the solution with Milli-Q water for the removal of adsorbed piece on the GCE. For the preparation of NiCo₂O₄ suspension, 3 mg of NiCo₂O₄, 0.1 ml Mill-Q water and 0.9 ml of N, N-Dimethyl formamide (DMF) were mixed. The prepared mixture was ultra-sonicated for 30 min in order to get the uniform suspension. 3

μl of resultant suspension was taken out using micro pipette and drop casted on the finely polished GCE surface and dried at room temperature.

3. Results and Discussion



Scheme 2: The electrocatalytic oxidation of hydrazine on the NiCo_2O_4 NR modified electrode.

3.1 XRD studies

The sample phase purity and crystal structure were confirmed by XRD. **Figure 1A** shows the XRD pattern of NiCo_2O_4 . The calcined NiCo_2O_4 diffraction peaks are found at 2θ values of $\sim 18.9^\circ$, $\sim 31.1^\circ$, $\sim 36.7^\circ$, $\sim 38.4^\circ$, $\sim 44.6^\circ$, $\sim 55.4^\circ$, $\sim 59.1^\circ$, $\sim 64.9^\circ$ and $\sim 77.0^\circ$ which can be indexed with (111), (220), (311), (222), (400), (422), (511), (440) and (533) planes and all the diffraction peaks are assigned in the cubic phase of NiCo_2O_4 . The observed diffraction pattern of NiCo_2O_4 matches with ICDD card data with a reference number of 01-073-1702. The observed XRD pattern was also in good agreement with the earlier reports [38]. No other impurity phase peak was observed which further substantiated the purity of sample. Thermal stability of NiCo_2O_4 was studied by TG analysis and the result is shown in **Figure 1B**. The first weight loss of about 3 % was observed below 150°C which indicating

the removal of physically and chemically adsorbed water (H_2O) content. A major weight loss was observed at the temperature range of ~ 300 °C to 370 °C which is attributed to the decomposition of Ni^{2+} and Co^{3+} . Therefore, 400 °C was chosen as the calcination temperature. **Figure S1A** shows Raman spectroscopy of NiCo_2O_4 which gives the information related to changes in structure and composition. The peak observed 691 cm^{-1} (A_{1g}) vibration corresponds to Oh oxygen ions in Co 3p present in Co_3O_4 , and other two peaks were located at 484 cm^{-1} and 523 cm^{-1} combined vibration of Td and Oh oxygen atoms in the lattice. The observed three peaks were more sensitive to Ni 2p ion substituted in Co_3O_4 spinel lattice. Hence, the peak at 691 cm^{-1} come to be weak and shifted to lower frequencies, when Ni 2p exchanged in Co 3p in the Oh sites [39]. From the above vibrational peaks confirms the formation of NiCo_2O_4 because the peak were observed at $660, 503, 460$ and 187 cm^{-1} corresponding to $A_{1g}, F_{2g}, E_g, F_{2g}$ and modes of NiCo_2O_4 [40,41]. **Figure S1B** shows FT-IR studies of NiCo_2O_4 . The peaks were observed at $555, 642\text{ cm}^{-1}$ correspond to M-O vibration of NiCo_2O_4 . The peak at 1366 cm^{-1} may be associated with physically adsorbed CO_2 . The peaks at 1636 and 3484 cm^{-1} corresponding to vibration mode of absorbed water molecules [42].

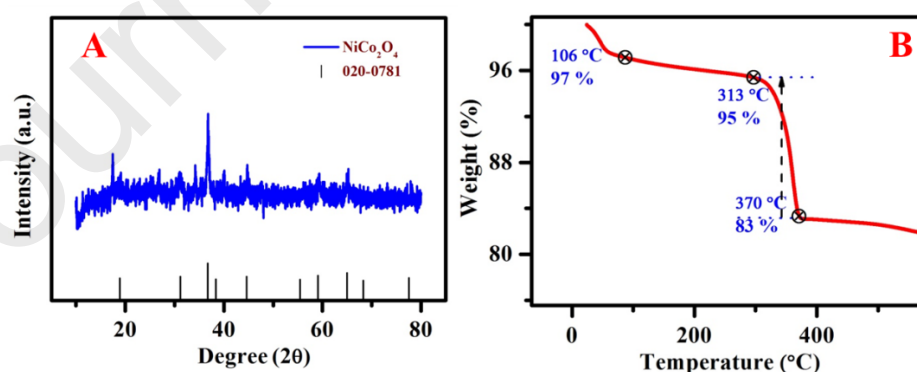


Figure 1 (A) XRD and (B) TGA of NiCo_2O_4 NR.

3.2 Morphological studies

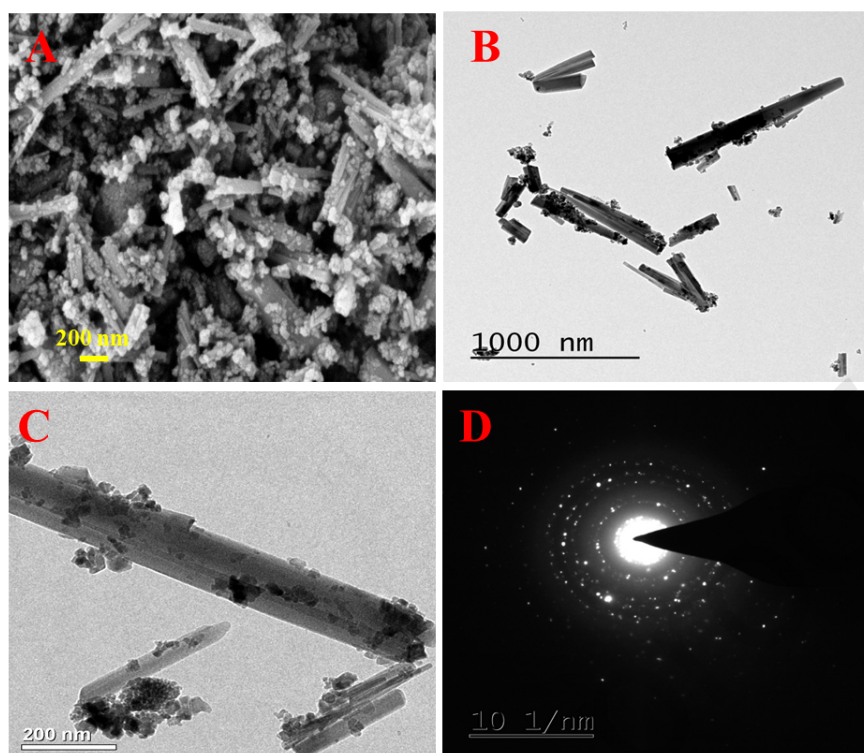


Figure 2 (A) FESEM; (B) TEM; (C) HRTEM images and (D) SAED pattern of NiCo₂O₄ NR.

The FESEM, TEM and HRTEM analysis were used as a tool to study the surface morphology, size of the nanostructure and SAED pattern of NiCo₂O₄ NR. **Figure 2A** gives the low magnification (FESEM) micrographs of the NiCo₂O₄ NR which shows that the as-synthesized material has broken nanorod as nanoparticle were situated on nanorod like structure. The TEM micrograph of the material was shown in **Figure 2B** where the NiCo₂O₄ NR micrograph was seen clearly. The observed morphological study, confirmed that the broken NR were situated on the NR. HRTEM morphology of NiCo₂O₄ NR was displayed in **Figure 2C**. **Figure 2D** displays a selected area electron diffraction (SAED) pattern of NiCo₂O₄ NR which clearly indicates that the NiCo₂O₄ NR was formed. The overall HRTEM and SAED results have clearly exposed the information about morphological, size and structure of the material.

Elemental mapping of NiCo_2O_4 NR is shown in **Figure 3A-D**. HRTEM micrograph of NiCo_2O_4 NR is shown in **Figure 3A** and insert of **Figure 3A** shows elemental mapping of all the three elements such as Ni, Co and O. **Figure 3 (B-D)** clearly display the elemental mapping of Ni, Co and O, respectively. These figures evidently confirm the formation of NiCo_2O_4 NR with well distribution of all three elements. The EDAX analysis also carried out using SEM techniques the result is shown in **Figure S2**. EDAX study also confirms the presence of Ni, Co and O elements without any other impurities.

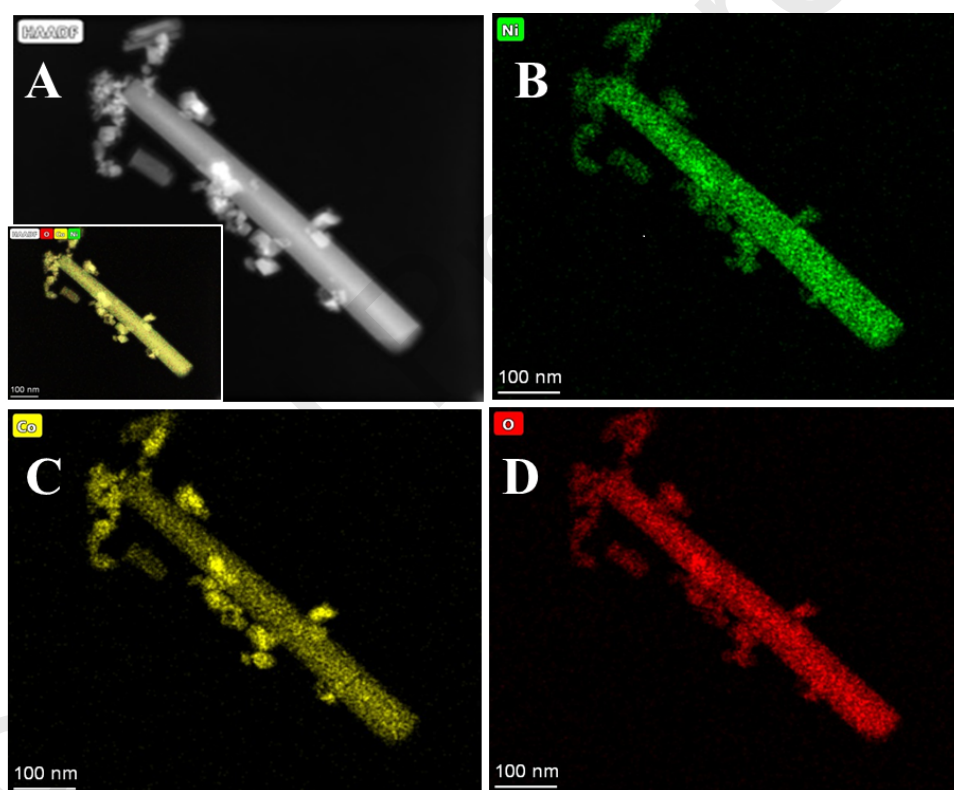


Figure 3 (A) HRTEM image; Elemental mapping of Ni (B), Co (C) and O (D) of NiCo_2O_4 NR.

3.3 X-ray photoelectron spectroscopic studies

The chemical composition, surface oxidation state and nature of the each component exist in the NiCo_2O_4 NR was analysed by XPS study. **Figure 4A** depicts the XPS survey spectrum of NiCo_2O_4 NR. Survey spectrum clearly identified the existence of Ni, Co and O without other impurities. Gaussian fitting method was used for the high magnification XPS studies of Co 2p, Ni 2p and O 1s spectrum which were shown in **Figures 4B-D**. **Figure 4B** shows that the fitted Ni 2p has two spin orbit doublets (Ni 2p_{3/2} and Ni 2p_{1/2} electronic configuration) two kind of Ni species has been found which are assigned to Ni²⁺ and Ni³⁺. Particularly, the peaks at the binding energies of 857.1 eV and 874.7 eV are characteristic of Ni³⁺ and the peaks observed at 855.3 eV and 872.9 eV correspond to Ni²⁺ [43].

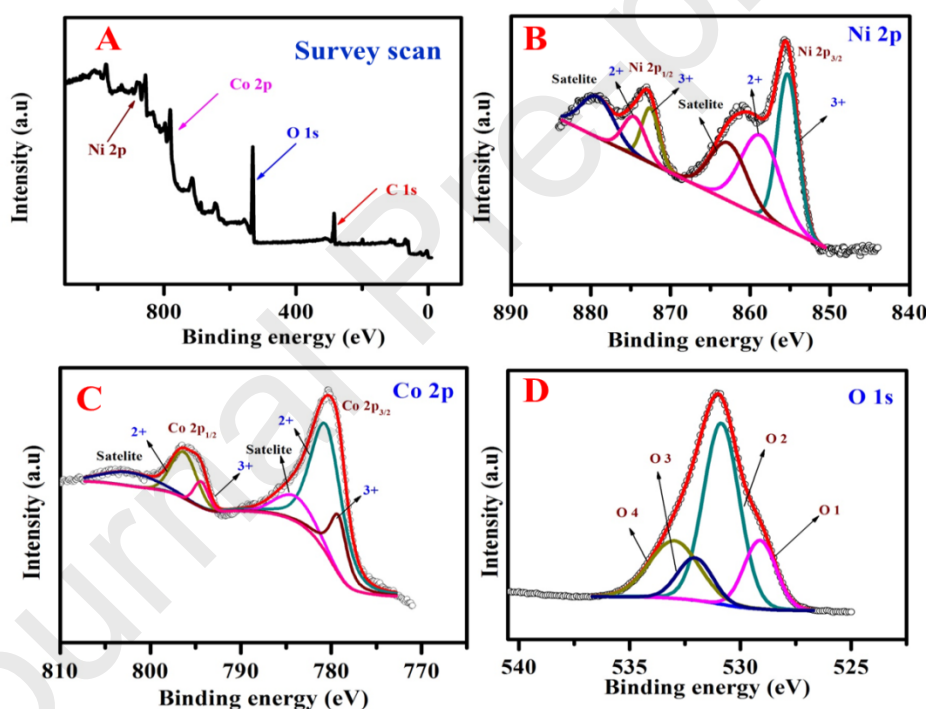


Figure 4 XPS study of NiCo_2O_4 NR (A) survey scan; (B) Ni 2p; (C) Co 2p and (D) O 1s.

The fitted Co 2p spectrum was displayed in **Figure 4C**. The Co 2p has two spin orbit doublets Co 2p_{3/2} and Co 2p_{1/2} electronic configuration at the binding energies of 779.4 eV and 794.3 eV corresponding to characteristic of Co²⁺ and Co³⁺, respectively. In this spectrum two shakeup satellite peaks (identified as “satellite”) were observed along with the two spin

orbit doublets [44]. The high resolution O 1s showed in **Figure 4D** exhibits four peaks at 529.3 eV (denoted as “O 1”), 530.7 eV (denoted as “O 2”), 531.8 eV (denoted as “O 3”) and 532.6 eV (denoted as “O 4”) was consigned to lattice oxygen in **NiCo₂O₄ NR**, oxygen in –OH, the defect sites with low oxygen coordination and chemisorbed/physisorbed water molecule on the surface respectively [43].

4. Electrochemical studies

4.1 Cyclic voltammetry comparison study

Cyclic voltammetric (CV) study was performed to assess the electrocatalytic behaviour of NiO/GCE, Co₃O₄/GCE and NiCo₂O₄ NR/GCE towards electro-oxidation of hydrazine as shown in **Figure S3**. This figure clearly displays that the NiCo₂O₄ NR demonstrates higher catalytic activity compared with NiO and Co₃O₄. **Figure 5** illustrates the CV of bare GCE and NiCo₂O₄ NR/GCE in the absence of hydrazine (curve ‘a’ and ‘b’) and the NiCo₂O₄ NR/GCE in the presence of 3 mM of hydrazine (curve ‘c’) in 0.1 M supporting electrolyte at a scan rate of 25 mV s⁻¹. The modified electrode shows abrupt increase in oxidation peak current value at much lower potential due to excellent electrocatalytic activity and high conductive nature of NiCo₂O₄ NR [16]. These observations intensely spotlight and indicate the electrocatalytic behaviour of modified electrode for hydrazine oxidation.

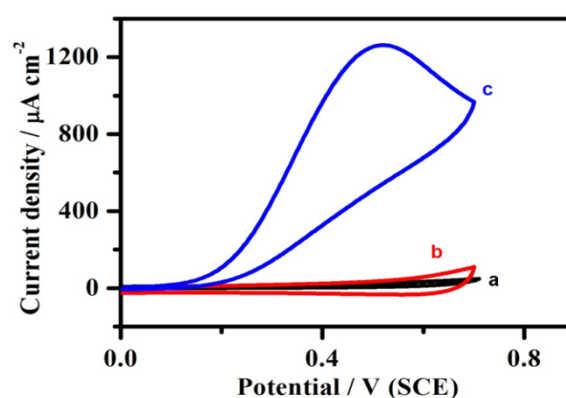


Figure 5 CV of bare GCE (a); NiCo₂O₄ NR/GCE in the absence of hydrazine (b) and NiCo₂O₄ NR/GCE in the presence of 3 mM hydrazine (c) at 25 mV s⁻¹.

4.2 pH effect

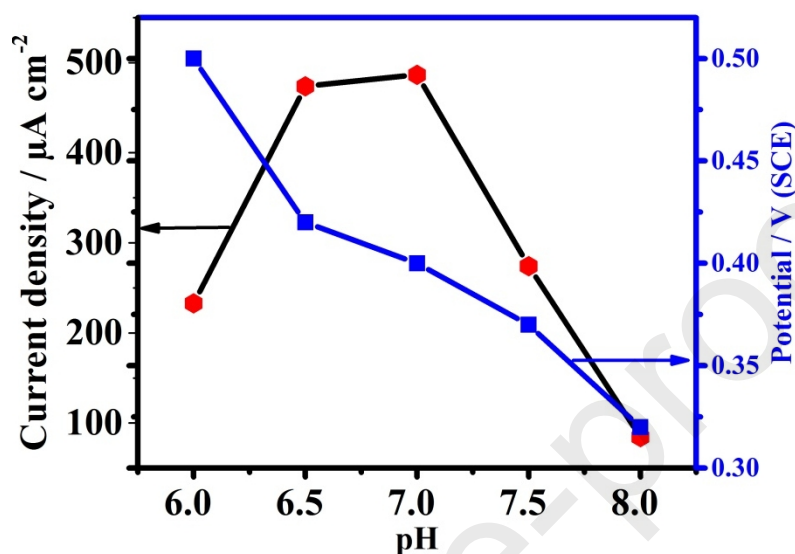


Figure 6 Effect of pH on peak current and peak potential for the electrooxidation of 2 mM of hydrazine at NiCo₂O₄ NR/GCE

Electrochemical oxidation of hydrazine depends on the solution pH. Due to this factor, optimisation of pH is essential for the efficient electrocatalytic detection of hydrazine.

Figure 6 shows as the pH of solution increases from 6.0, the peak current increases and peak potential shifts towards negative direction. The maximum peak current was observed at pH=7. Hence, pH 7 was chosen as optimum pH in the present study for the detection of hydrazine.

4.3 Effect of scan rate

In order to get the information on kinetics of electrochemical oxidation of hydrazine oxidation on NiCo₂O₄ NR/GCE, CV measurements were performed in 0.1 M PBS containing 3 mM of hydrazine at different scan rates as shown in **Figure S4A**. As shown in **Figure S4B**,

the anodic oxidation current increased linearly with square root of scan rate. Also, the slope of $\log(\text{peak current})$ vs $\log(\text{scan rate})$ plot (**Figure S4C**) was found to be nearly 0.5. These results explicitly show that the electrooxidation of hydrazine was controlled by the diffusion of electroactive species (i.e., hydrazine) from bulk to the electrode/electrolyte interface and the rate of electron transfer between the modified electrode and hydrazine is fast [45].

4.4 Effect of concentration

Figure 7A displays the catalytic performance of **NiCo₂O₄ NR/GCE** in various concentration of **hydrazine**. The oxidation peak was observed at 0.36 V and the oxidation peak current value also increased linearly with increase in the concentration of **hydrazine** from 0.07 to 6.0 mM. The corresponding current density vs. concentration plot is shown in **Figure 7B**. From the calibration plot, the linear range and sensitivity with correlation coefficient $R^2=0.998$ were found to be 0.07 to 1.78 mM, $290 \mu\text{A cm}^{-2} \text{mM}^{-1}$, respectively. The DPV of **NiCo₂O₄ NR/GCE** is shown in **Figure 7C** which showed that the anodic oxidation of **hydrazine** was observed at 0.25 V with respect to **NiCo₂O₄ NR/GCE**. Increasing the concentration of **hydrazine** the oxidation current value increases correspondingly. **Figure 7D** shows a plot of current density vs. the **hydrazine** concentration, which depicts linear correlation in the range of 0.01 to 2.25 mM. The best linear fitted equation $j_p (\mu\text{A}) = 48.25 \pm 1.6 (\text{mM}) + 2.56 \pm 1.8$ with a correlation coefficient $R^2 = 0.989$. The sensitivity and detection limit (LOD) were $48.25 \mu\text{A cm}^{-2} \text{mM}^{-1}$ and $0.26 \mu\text{M}$, respectively. Limit of qualification (LOQ) ($10 \times \text{standard deviation/slope}$) is $0.874 \mu\text{M}$. As shown in **Table 1**, the analytical factors such as sensitivity, linear range and detection limit concerning the sensing of **hydrazine** using **NiCo₂O₄ NR/GCE** which is compared with previous reports [46-54] based on various sensors. From the above table we can conclude that **NiCo₂O₄ NR** is a suitable catalyst for the **hydrazine** sensing.

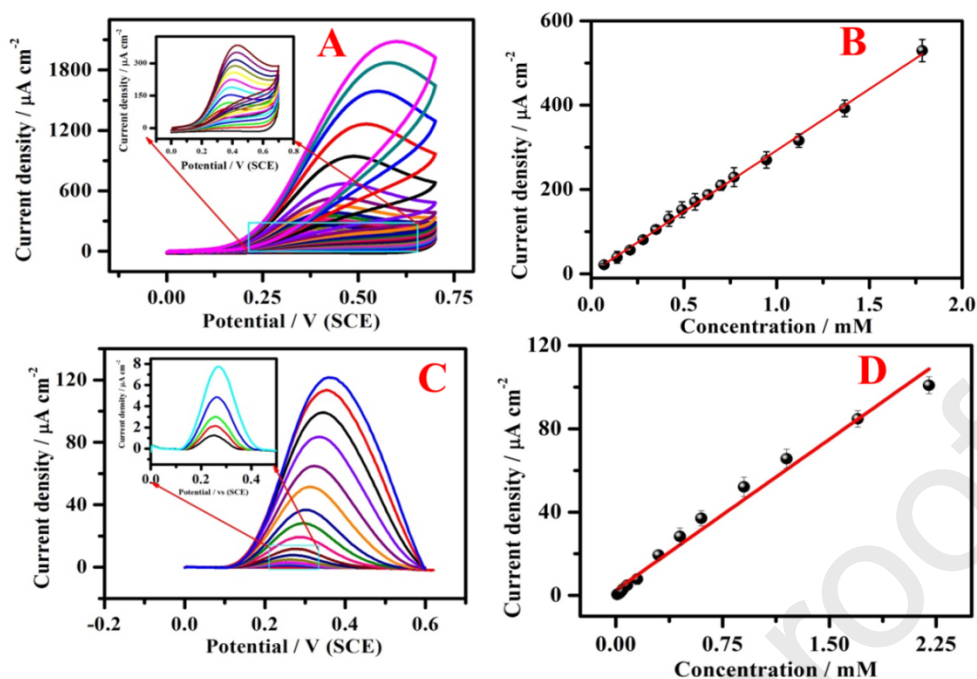


Figure 7 (A) CV response of NiCo₂O₄ NR/GCE in different concentration (0.07, 0.14, 0.21, 0.28, 0.35, 0.42, 0.49, 0.56, 0.63, 0.70, 0.77, 0.945, 1.12, 1.67, 1.78, 3.0, 4.0, 5.0 and 6.0 mM) of hydrazine; (B) A plot of j_{pa} vs. [hydrazine]; Scan rate at 5 mV s⁻¹; (C) DPV of NiCo₂O₄ NR modified electrode in hydrazine concentration range from 0.01 mM to 2.25 mM at the NiCo₂O₄ NR/GCE and (D) corresponding calibration curve.

Table 1 Comparison of the analytical performance of NiCo₂O₄ NR modified electrode with other sensors for the electrochemical hydrazine detection.

Sensor techniques	Linear range (μM)	Sensitivity	Limit of detection (μM)	Reference
Colorimetric sensor	6.0-40.0	-	1.1	[46]
	0.5-20.0	-	0.4	[47]
Chromatography	500-10000	-	20	[48]
	0.17-50	-	0.17	[49]

Fluorescence sensor	0.2-9.3	-	0.08	[50]
Electrochemical sensor	2.4-820	-	1.0	[51]
	0-1200	75 $\mu\text{A mM}^{-1}$	40	[52]
	0.07-500	-	0.04	[53]
	0.2-50	136.2 $\mu\text{A mM}^{-1}$ $^1\text{cm}^{-2}$	0.07	[54]
	3.0-300	-	1.0	[6]
	0.25-3400	270.0 $\mu\text{A mM}^{-1}$ $^1\text{cm}^{-2}$	0.06	[55]
	0.05-1600	1.95 $\mu\text{A mM}^{-1}$ cm^{-2}	0.028	[56]
	5.0-1300	449.7 $\mu\text{A mM}^{-1}$ $^1\text{cm}^{-2}$	1.4	[57]
	10-2250	48.25 $\mu\text{A mM}^{-1}$ $^1\text{cm}^{-2}$	0.26	Present work

As shown in **Table 1**, the analytical factors including sensitivity, linear range and limit of detection of NiCo_2O_4 NR/GCE are comparable with previous reports [46-54] based on various techniques. From the above table we can conclude that NiCo_2O_4 NR is a suitable catalyst for the electrochemical sensing of hydrazine.

4.5 Real sample analysis

In order to check the practical use of the proposed sensor (NiCo_2O_4 NR/GCE), hydrazine detection was carried out with different water samples. The as-collected water

samples from Karaikudi city, Tamil Nadu were tested for hydrazine concentration level in water without further pretreatment by proposed sensor technique. As collected water samples are found to be free from hydrazine (no peak response/signal) therefore, externally particular amount of hydrazine was spiked into the collected water samples to make the water contaminated. Following standard addition method the recoveries were examined by the catalytic current response corresponding results were displayed in Table 2. The observed results present reliable recovery with acceptable RSD values which indicates that our NiCo₂O₄ NR/GCE could be a potential candidate for the detection of hydrazine in practical purpose.

Table 2 Real sample analysis of hydrazine in real water samples by NiCo₂O₄ NR/GCE.

Samples	Detected	Added (μM)	Found ^s (μM)	Recovery (%)	RSD (%)
Sample 1	-	150	147	98.0	4.1
Sample 2	-	120	118	98.6	2.6

^s-Standard addition method

4.6 Reproducibility and stability studies

Figure 8A shows the differential pulse voltammogram response recorded for the selectivity of hydrazine sensor and several common coexisting interfering substances (Cd²⁺, Pb²⁺, CaCl₂, NaNO₃, KCl, NaSO₄ and MgCl₂). The oxidation response was recorded for hydrazine and 20 times higher concentration of interferents. The outcome result depicts that no obvious current changes were observed for the interference. Hence, the interferents are not affecting the hydrazine oxidation. From this result we can conclude that our proposed sensor has excellent selectivity towards the detection of hydrazine. The stability of the sensor was

examined by cyclic voltammetry study. The NiCo_2O_4 NR shows good stability for the detection of hydrazine by retaining 89 % of the initial response after 50 cycles.

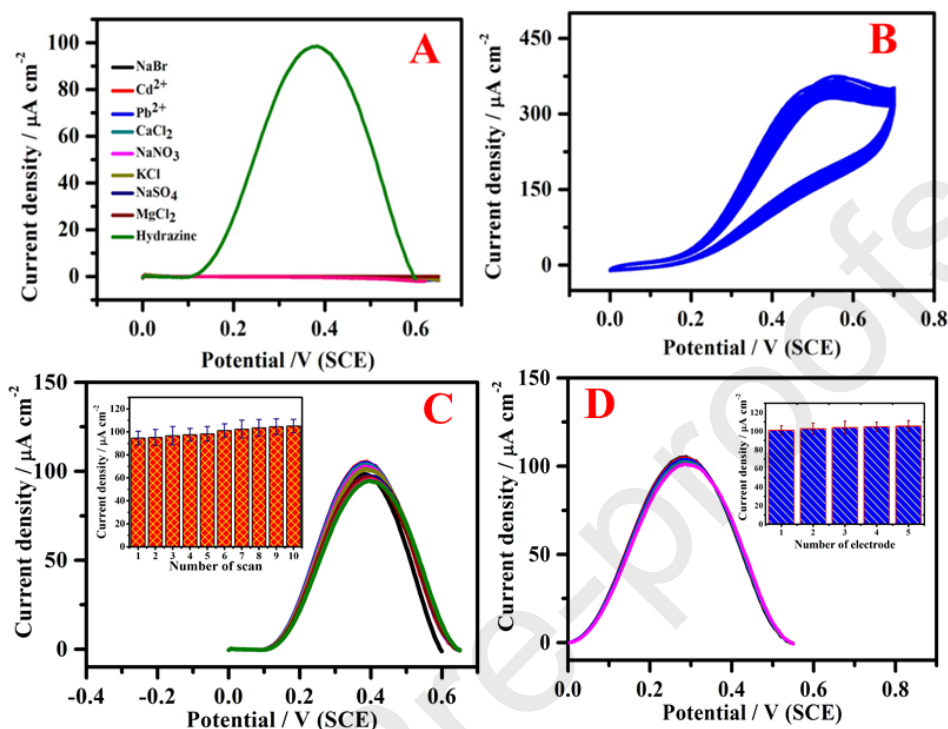


Figure 8 (A) Differential pulse voltammogram current response of NiCo_2O_4 NR for 0.02 M of hydrazine, 0.4 M of Cd^{2+} , Pb^{2+} , CaCl_2 , NaNO_3 , KCl, NaSO_4 and MgCl_2 interferences into 0.1 M PBS; (B) Cyclic voltammogram responses of the NiCo_2O_4 NR to 2 mM hydrazine in 0.1 M PBS (pH=7) for 50 cycles. Scan rate: 25 mV s^{-1} ; (C) and (D) Differential pulse voltammogram of repeatability and fabrication reproducibility of NiCo_2O_4 NR modified electrode.

Reproducibility of the NiCo_2O_4 NR modified electrode for hydrazine determination was investigated using DPV. As shown in **Figure 8B**, the stability (50 cycles) of the modified electrode was examined in the presence of 2 mM of hydrazine at the scan rate of 25 mV s^{-1} . The relative standard deviation RSD was 4 %. Repeatability of the sensor was examined by repeating the measurement ten times with 5 mins interval of time and the results are displayed in **Figure 8C**. The peak current value and peak potential occurred at similar

position. The RSD value = 3.9 %. It indicates that our NiCo₂O₄ NR/GCE sensor has excellent repeatability for the electrooxidation of hydrazine. Finally, fabrication reproducibility (Figure 8D) (inter electrode) was examined by preparing five modified electrodes with same fabrication condition. All the electrodes gave excellent fabrication reproducibility with the RSD value of 1.6 %. From the above results we can conclude that our fabricated sensor has excellent reproducibility, stability, repeatability and selectivity.

5. Conclusion

In conclusion, NiCo₂O₄ NR has been synthesized by a simple hydrothermal approach. It has been characterized by several physiochemical and electrochemical techniques. XPS study confirms the formation of NiCo₂O₄ NR and the oxidation state of the material. The HRTEM study reveals that our synthesized material was NR like structure. In view of their unique structural advantage and electrochemical performance, the possibility of employing NiCo₂O₄ NR for the detection of hydrazine was carefully investigated. NiCo₂O₄ NR shows efficient catalytic performance for the detection of hydrazine with wide linear range and low limit of detection. The NiCo₂O₄ NR shows higher electrocatalytic activity for the detection of hydrazine oxidation compared with bare electrode. The proposed sensor depicts good sensitivity (48.25 $\mu\text{A cm}^{-2} \text{mM}^{-1}$), low LOD (260 nm), stability, reproducibility and selectivity. As-synthesised NiCo₂O₄ NR was used as a modified electrode in the field of analytical uses for the sensing of hydrazine in the analysed water samples. Hence, this work provides simple and efficient method for the sensing of hydrazine.

Acknowledgment

We thank the CSIR and UGC, New Delhi for the award of a UGC-Senior Research Fellowship for Mrs.V. Sudha. We wish to acknowledge the Central Instrumentation Facility (CIF), CSIR-CECRI, Karaikudi for characterization studies.

References

- [1] S.K. Mehta, K. Singh, A. Umar, G.R. Chaudhary, S. Singh, *Electrochim. Acta* 69 (2012) 128–133.
- [2] Y.J. Yang, W. Li, X. Wu, *Electrochim. Acta* 123 (2014) 260–267.
- [3] R. Madhu, B. Dinesh, S.M. Chen, R. Saraswathi, V. Mani, *RSC Adv.* 5 (2015) 54379–54386.
- [4] Y.Y. Tang, C.L. Kao, P.Y. Chen, *Anal. Chim. Acta* 711 (2012) 32–39.
- [5] P. Muthukumar, S.A. John, *J. Solid State Electrochem.* 18 (2014) 2393–2400.
- [6] C. Wang, L. Zhang, Z. Guo, J. Xu, H. Wang, K. Zhai, X. Zhuo, *Microchim. Acta* 169 (2010) 1–6.
- [7] E. Vernot, *Fundam. Appl. Toxicol.* 5 (1985) 1050–1064.
- [8] J.W. Mo, B. Ogorevc, X. Zhang, B. Pihlar, *Electroanalysis* 12 (2000) 48–54.
- [9] S. Amlathe, V.K. Gupta, *Analyst* 113 (1988) 1481–1483.
- [10] K. Ravichandran, R.P. Baldwin, *Anal. Chem.* 55 (1983) 1782–1786.
- [11] A. Ensafi, *Talanta* 47 (1998) 645–649.
- [12] Y.Y. Liu, I. Schmeltz, D. Hoffmann, *Anal. Chem.* 46 (1974) 885–889.
- [13] M. Michlmayr, D.T. Sawyer, *J. Electroanal. Chem. Interfacial Electrochem.* 23 (1969) 375–385.
- [14] C. Karuppiyah, M. Velmurugan, S.-M. Chen, R. Devasenathipathy, R. Karthik, S.-F. Wang, *Electroanalysis* 28 (2016) 808–816.

- [15] R. Devasenathipathy, V. Mani, S.-M. Chen, *Talanta* 124 (2014) 43–51.
- [16] C. Yuan, H. Bin Wu, Y. Xie, X.W.D. Lou, *Angew. Chemie Int. Ed.* 53 (2014) 1488–1504.
- [17] S. and Y.N. O. Knop, K. I. G. Reid, *Can. J. Chem.* 46 (1968) 3463–3476.
- [18] P.D. Battle, A.K. Cheetham, J.B. Goodenough, *Mater. Res. Bull.* 14 (1979) 1013–1024.
- [19] B. Kaur, B. Satpati, R. Srivastava, *New J. Chem.* 39 (2015) 1115–1124.
- [20] X.Y. Yu, X.Z. Yao, T. Luo, Y. Jia, J.H. Liu, X.J. Huang, *ACS Appl. Mater. Interfaces* 6 (2014) 3689–3695.
- [21] W. Huang, Y. Cao, Y. Chen, J. Peng, X. Lai, J. Tu, *Appl. Surf. Sci.* 396 (2017) 804–811.
- [22] S. Liu, J. Wu, J. Zhou, G. Fang, S. Liang, *Electrochim. Acta* 176 (2015) 1–9.
- [23] T.H. Ko, K. Devarayan, M.K. Seo, H.Y. Kim, B.S. Kim, *Sci. Rep.* 6 (2016) 1–9.
- [24] J. Li, S. Xiong, Y. Liu, Z. Ju, Y. Qian, *ACS Appl. Mater. Interfaces* 5 (2013) 981–988.
- [25] L. Qian, L. Gu, L. Yang, H. Yuan, D. Xiao, *Nanoscale* 5 (2013) 7388–7396.
- [26] G. Zhang, X.W.D. Lou, *Sci. Rep.* 3 (2013) 2–7.
- [27] L. Yu, G. Zhang, C. Yuan, X.W. Lou, *Chem. Commun.* 49 (2013) 137–139.
- [28] G.Q. Zhang, H. Bin Wu, H.E. Hoster, M.B. Chan-Park, X.W. Lou, *Energy Environ. Sci.* 5 (2012) 9453–9456.
- [29] G. Zhang, X.W.D. Lou, *Adv. Mater.* 25 (2013) 976–979.

- [30] M.U. Anu Prathap, R. Srivastava, *Electrochim. Acta* 108 (2013) 145–152.
- [31] T.-H. Ko, K. Devarayan, M.-K. Seo, H.-Y. Kim, B.-S. Kim, *Sci. Rep.* 6 (2016) 20313.
- [32] Y. Mo, Q. Ru, J. Chen, X. Song, L. Guo, S. Hu, S. Peng, *J. Mater. Chem. A* 3 (2015) 19765–19773.
- [33] J. Wu, R. Mi, S. Li, P. Guo, J. Mei, H. Liu, W.M. Lau, L.M. Liu, *RSC Adv.* 5 (2015) 25304–25311.
- [34] W. Zhou, D. Kong, X. Jia, C. Ding, C. Cheng, G. Wen, *J. Mater. Chem. A* 2 (2014) 6310–6315.
- [35] X. Liu, S. Shi, Q. Xiong, L. Li, Y. Zhang, H. Tang, C. Gu, X. Wang, J. Tu, *ACS Appl. Mater. Interfaces* 5 (2013) 8790–8795.
- [36] Y. Lei, J. Li, Y. Wang, L. Gu, Y. Chang, H. Yuan, D. Xiao, *ACS Appl. Mater. Interfaces* 6 (2014) 1773–1780.
- [37] G.-Y. Zhang, B. Guo, J. Chen, *Sensors Actuators B Chem.* 114 (2006) 402–409.
- [38] M. Kundu, G. Karunakaran, E. Kolesnikov, V.E. Sergeevna, S. Kumari, M. V. Gorshenkov, D. Kuznetsov, *J. Ind. Eng. Chem.* 59 (2018) 90–98.
- [39] C.F. Windisch, G.J. Exarhos, R.R. Owings, *V J. Appl. Phys.* 95 (2004) 5435–5442.
- [40] W. Xiong, Y. Gao, X. Wu, X. Hu, D. Lan, Y. Chen, X. Pu, Y. Zeng, J. Su, Z. Zhu, *ACS Appl. Mater. Interfaces.* 6 (2014) 19416–19423.
- [41] E. Umeshbabu, G. Rajeshkhanna, P. Justin, G.R. Rao, *Mater. Chem. Phys.* 165 (2015) 235–244.
- [42] G. Karunakaran, M. Jagathambal, M. Venkatesh, G. Suresh Kumar, E. Kolesnikov, A.

- Dmitry, A. Gusev, D. Kuznetsov, *Powder Technol.* 305 (2017) 488–494.
- [43] C. Yuan, J. Li, L. Hou, X. Zhang, L. Shen, X.W.D. Lou, *Adv. Funct. Mater.* 22 (2012) 4592–4597.
- [44] B. Cui, H. Lin, Y. Liu, J. Li, P. Sun, X. Zhao, C. Liu, *J. Phys. Chem. C* 113 (2009) 14083–14087.
- [45] J. Wu, T. Zhou, Q. Wang, A. Umar, *Sensors Actuators B Chem.* 224 (2016) 878–884.
- [46] B. Zargar, A. Hatamie, *Sensors Actuators B Chem.* 182 (2013) 706–710.
- [47] Y. He, W. Huang, Y. Liang, H. Yu, *Sensors Actuators B Chem.* 220 (2015) 927–931.
- [48] G. Elias, W.F. Bauer, *J. Sep. Sci.* 29 (2006) 460–464.
- [49] J. Zhang, L. Ning, J. Liu, J. Wang, B. Yu, X. Liu, X. Yao, Z. Zhang, H. Zhang, *Anal. Chem.* 87 (2015) 9101–9107.
- [50] X. Chen, Y. Xiang, Z. Li, A. Tong, *Anal. Chim. Acta* 625 (2008) 41–46.
- [51] S.J.R. Prabakar, S.S. Narayanan, *J. Electroanal. Chem.* 617 (2008) 111–120.
- [52] K.K. Lee, P.Y. Loh, C.H. Sow, W.S. Chin, *Biosens. Bioelectron.* 39 (2013) 255–260.
- [53] H. Beitollahi, S. Tajik, S. Jahani, *Electroanalysis* 28 (2016) 1093–1099.
- [54] X. Gu, X. Li, S. Wu, J. Shi, G. Jiang, G. Jiang, S. Tian, *RSC Adv.* 6 (2016) 8070–8078.
- [55] Y. Dong, Z. Yang, Q. Sheng, J. Zheng, *Colloids Surfaces A Physicochem. Eng. Asp.* 538 (2018) 371–377.
- [56] S. Sakthinathan, S. Kubendhiran, S.M. Chen, P. Sireesha, C. Karupiah, C. Su,

Electroanalysis 29 (2017) 587–594.

[57] Z. Yang, Q. Sheng, S. Zhang, X. Zheng, J. Zheng, *Microchim. Acta* 184 (2017) 2219–2226.

Journal Pre-proofs

NiCo₂O₄ Nanorod: Synthesis and Electrochemical Sensing of Carcinogenic Hydrazine

Velayutham Sudha ^{a,b}, Sakkarapalayam Murugesan Senthil Kumar ^{a,b}, Rangasamy Thangamuthu ^{a, b*}

^a Materials Electrochemistry Division (MED), CSIR-Central Electrochemical Research Institute (CSIR-CECRI), Karaikudi-630 003, Tamil Nadu, India.

^b Academy of Scientific and Innovative Research (AcSIR), CSIR-Central Electrochemical Research Institute, Karaikudi- 630 003, Tamil Nadu, India.

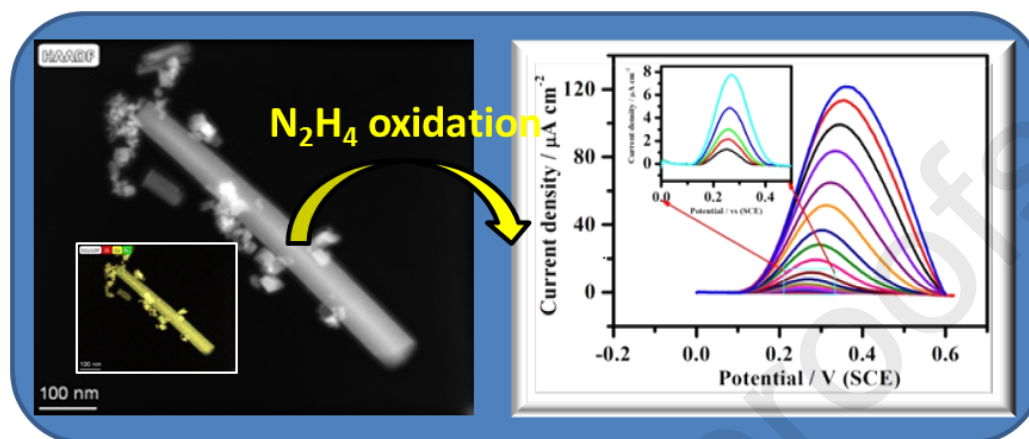
* To whom correspondence should be addressed. E-mail: thangamuthu@cecri.res.in; thangamuthu_r@yahoo.co.uk; Phone: +91-04565-241-350.

Abstract

In this work, we explored a simple hydrothermal process to tune the NiCo₂O₄ morphology into well defined rod structure with nanoparticle on it. The as prepared NiCo₂O₄ was characterized by various characterization studies such as XRD, Raman, FT-IR, TGA and HRTEM. The electrochemical sensing of hydrazine on NiCo₂O₄ nanorod was examined by cyclic voltammetry and differential pulse voltammetry techniques. The NiCo₂O₄ shows excellent electrocatalytic performance for the anodic oxidation of hydrazine. Interestingly, NiCo₂O₄ retain considerable current response after 50 cycles at 25 mV s⁻¹. The Ni and Co in bimetal oxides enhanced the current response due to their electroactive sites. The developed NiCo₂O₄ not only enhanced the current response of hydrazine but also exhibits good stability. NiCo₂O₄ demonstrates excellent detection limit and sensitivity of 260 nM and 48.25 $\mu\text{A cm}^{-2}$

mM⁻¹, respectively. For practical application, NiCo₂O₄/GCE was used for the sensing of hydrazine in real water samples.

Key words: Hydrazine, NiCo₂O₄, Hydrothermal method, Electrochemical sensing.



Scheme 1. Schematic illustration of NiCo₂O₄ characterization and electrochemical sensing of hydrazine.

1. Introduction

Hydrazine is widely used in fuel cell, food production, pharmaceutical intermediates, rocket fuel, pesticides production, blowing agent, dye industries, oxygen scavengers and so on [1–5]. The Environmental Protection Agency (EPA) identified hydrazine as a poisonous chemical and the proposed level in the commercial effluents is 1 ppm. Due to volatile nature of hydrazine, it is easily adsorbed on the human skin and damage the living organism especially, liver, blood production system and kidney [6]. Vernot et al., found that exposure to hydrazine for long time causes inhalation problem in different animals. Rats, hamsters, mice and dog were analysed post exposure of 18 months, 1 year, 15 months, 38 months, respectively. Male and female rats disclose dose-dependent prevalence of well-disposed nasal adenomatous polyps and smaller numbers of malignant nasal epithelial tumours after 1 year of exposure to hydrazine and 18 months post exposure holding [7], DNA damage [8] and

irreversible deterioration of nervous system [9]. Due to large consumption in industrial use, hydrazine and derivatives are commonly detected in atmosphere and it creates health hazardous particularly, in human. Nowadays, numerous methods are available to extensively detect the concentration of hydrazine including spectrophotometry [9], potentiometry [8], chemiluminescence [10], fluorimetry [11], gas chromatography-mass spectrometry [12], coulometry [13] and electrochemical method [14]. Compared with other method, electrochemical technique possesses many advantages including high sensitivity, portable, cost effective and simple operating procedure. Additionally, electrochemical method is a good modest substitute for the detection of hydrazine. Bare electrode suffers the disadvantages of high over potential and low sensing ability (signals) [15]. Commonly, the electrode surface was modified with nanostructured metal oxides, bimetal oxides, material possessing high surface area, catalytic activity and conductivity which improve the sensing signals of the analytes. Metal oxides are one of the investigated nanomaterials in the case of biotic and industrial applications due to their redox properties and catalytic activity. Mixed MOs are single phase bi-MOs consist of nickel and cobalt cations which have excellent electrocatalytic activity due to its synergetic effect in the case of mixed valence state and complex chemical composition either than the combination of nickel oxide and cobalt oxide [16]. The spinel NiCo_2O_4 is a transition metal oxide which has high theoretical capacity, excellent electrical conductivity, easy preparation procedure, easily controllable morphologies and environmental friendly. NiCo_2O_4 adopts the pure spinel form in their all the nickel (Ni) ions occupies octahedral (Oh) site and Co ions occupy both tetrahedral (Td) and Oh sites [17,18].

Recently, researchers reported that the NiCo_2O_4 modified electrode were used for the sensing of various bioanalytes and environmental pollutants such as ascorbic acid, uric acid, dopamine, glucose, lead and cadmium [19–21]. Due to their good electronic conductivity in

the form of mixed valences of Ni and Co cations is a beneficial for the fast electron transfer and it has excellent redox activity than to NiO and Co₃O₄ [16,22,23]. For the reason that, NiCo₂O₄ has atleast two order of higher magnitude than nickel oxide and cobalt oxide hence, it possess potential applications in the field of lithium ion batteries, supercapacitor, electrocatalyst optoelectronic devices and electrochemical sensor [24–30]. Prathap et al., already reported that NiCo₂O₄ was used for the detection of lindane which provides excellent sensing ability than single component oxides [30]. Recently, many methods are there for the preparation of NiCo₂O₄ nanomaterials with several structures which include nanoparticles, nanowire, nanoneedle, nanosheet, nanoflake and nanoflower [31–36]. The spinel oxides which has cobalt such as CuCo₂O₄, MnCo₂O₄, NiCo₂O₄, ZnCo₂O₄, MgCo₂O₄, etc. exhibit great attention due to their physicochemical properties, technological applications, sensors to electrode materials, catalysts and electrochemical devices [37]. In the present work, a hydrazine sensor was successfully developed using NiCo₂O₄ broken nanorod as nanoparticle were situated on NR. NiCo₂O₄ NR/GCE shows pronounced performance for the detection of hydrazine in terms of sensitivity, selectivity, reproducibility and stability. There are no reports available for the detection of hydrazine using NiCo₂O₄ NR modified electrode.

2. Experimental section

2.1. Materials

CoCl₂.6H₂O, NiCl₂.6H₂O, urea were purchased from Merck. Disodium hydrogen phosphate (Na₂HPO₄) and monosodium hydrogen phosphate (NaH₂PO₄) purchased from Sigma Aldrich. These chemicals were used to prepare the phosphate buffer supporting electrolyte solution (PBS) throughout the electrochemical measurements. All the chemicals were used directly without any other purification. Throughout the study, Milli-Q water with a resistivity of 18.2 MΩ collected from Mill-Q instrument. The collected Milli-Q water was used for the experimental solution preparations.

2.2. Synthesis of nanostructured NiCo₂O₄

NiCo₂O₄ was prepared by hydrothermal method. Initially, 1 g of CoCl₂.6H₂O and 0.5 g of NiCl₂.6H₂O and 1 g of urea were dissolved in 30 mL of deionized (DI) water and stirred continuously until pink colour was observed. The transparent pink solution was transferred to the Teflon lined stainless autoclave. The sample was heated at 130 °C for 6 hrs. Then, the solution was cool down to room temperature followed by washing with DI water and ethanol for more than five times. The sample was dried in vacuum over at 80 °C for 6 hrs. To end, the powdered sample was calcined 400 °C under air atmosphere at a heating rate of 5 °C/min for 3 hrs. The absolute products were examined and used for electrochemical studies. Similar procedure was followed for the synthesis of NiO and Co₃O₄.

2.3. Characterizations

The sample phase purity of the NiCo₂O₄ material was examined by X-ray diffraction (XRD) studies by Cu K α radiation ($\lambda = 0.15$ nm using Bruker D8 ADVANCE X-ray diffractometer within the range of 10 – 80°. Thermogravimetric analysis (TGA), by TGA/DTA system (Model of SDT Q600), was performed to explore the material decomposition temperature in the heating range of 0 °C to 590 °C in an open airspace. Fourier transform infra-red (FT-IR) spectroscopy for powder sample was accomplished by KBr pellet method using Bruker Optik GmbH, Germany Model No: TENSOR 27 in the scale from 400 to 4000 cm⁻¹. Raman spectroscopic study was examined by He–Ne laser (wavelength $\lambda = 633$ nm) using RENISHAW I laser Raman microscope in order to understand the chemical behaviour of the material. The chemical composition (EDAX) of the prepared samples was characterized by scanning electron microscope using TESCAN (Supra 55VP) operating at an accelerating voltage of 30 kV. NiCo₂O₄ was studied by Field emission scanning electron microscopy (FESEM) (Oxford instrument). The structural features were

studied by transmission electron microscopy (TEM; JEOL-JEM 2010 and TecnaiTM G² F20, FEI which operate with an accelerating voltage of 200 kV) The structural features of the material were observed using high resolution transmission electron microscopy (HRTEM; TecnaiTM G² TF20 working at an accelerating voltage of 200 kV). Elemental compositions and survey scan of the prepared NiCo₂O₄ material was probed using Mg K α (1253.6 eV) as X-ray source (Thermo Scientific, MULTILAB 2000) via X-ray photoelectron spectroscopy (XPS) using Theta Probe AR-XPS system.

2.4. Electrochemical measurement

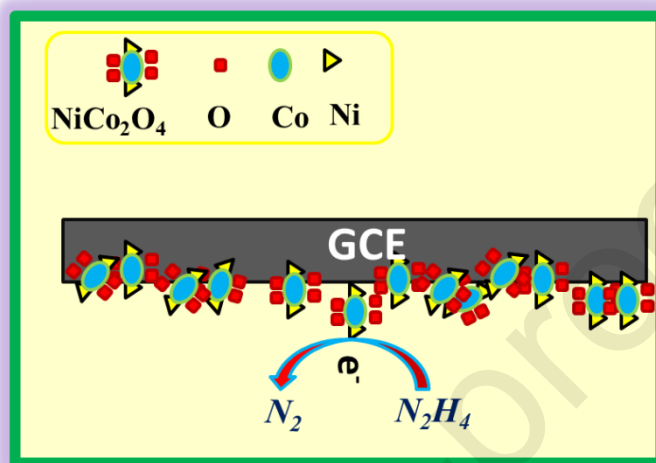
The hydrazine sensing performance of NiCo₂O₄ was studied using differential pulse voltammetry (DPV) and cyclic voltammetry (CV) techniques by AUTOLAB PGSTAT302N using three electrodes system with cleaned glassy carbon electrode (GCE; 3 mm diameter electrode geometric area=0.07 cm²) as working electrode, platinum electrode as counter electrode and Hg/HgCl₂/KCl_(sat) (saturated calomel electrode (SCE)) was used as reference electrode. Highly-pure N₂ gas used to purge into the experimental suspension before initiation of each experiments in order to remove the dissolved O₂ in the PBS (0.1 M, pH = 7). The electrocatalytic behaviour of NiCo₂O₄ NR/GCE towards oxidation of hydrazine was examined at room temperature.

2.5. Preparation of NiCo₂O₄ NR/GCE

Prior to the modification, bare GCE was polished with alumina slurry subsequently rinsed thoroughly in Mill-Q water and ultra-sonicate the solution with Milli-Q water for the removal of adsorbed piece on the GCE. For the preparation of NiCo₂O₄ suspension, 3 mg of NiCo₂O₄, 0.1 ml Mill-Q water and 0.9 ml of N, N-Dimethyl formamide (DMF) were mixed. The prepared mixture was ultra-sonicated for 30 min in order to get the uniform suspension. 3

μl of resultant suspension was taken out using micro pipette and drop casted on the finely polished GCE surface and dried at room temperature.

3. Results and Discussion



Scheme 2: The electrocatalytic oxidation of hydrazine on the NiCo₂O₄ NR modified electrode.

3.1 XRD studies

The sample phase purity and crystal structure were confirmed by XRD. **Figure 1A** shows the XRD pattern of NiCo₂O₄. The calcined NiCo₂O₄ diffraction peaks are found at 2θ values of $\sim 18.9^\circ$, $\sim 31.1^\circ$, $\sim 36.7^\circ$, $\sim 38.4^\circ$, $\sim 44.6^\circ$, $\sim 55.4^\circ$, $\sim 59.1^\circ$, $\sim 64.9^\circ$ and $\sim 77.0^\circ$ which can be indexed with (111), (220), (311), (222), (400), (422), (511), (440) and (533) planes and all the diffraction peaks are assigned in the cubic phase of NiCo₂O₄. The observed diffraction pattern of NiCo₂O₄ matches with ICDD card data with a reference number of 01-073-1702. The observed XRD pattern was also in good agreement with the earlier reports [38]. No other impurity phase peak was observed which further substantiated the purity of sample. Thermal stability of NiCo₂O₄ was studied by TG analysis and the result is shown in **Figure 1B**. The first weight loss of about 3 % was observed below 150 °C which indicating

the removal of physically and chemically adsorbed water (H_2O) content. A major weight loss was observed at the temperature range of ~ 300 °C to 370 °C which is attributed to the decomposition of Ni^{2+} and Co^{3+} . Therefore, 400 °C was chosen as the calcination temperature. **Figure S1A** shows Raman spectroscopy of $NiCo_2O_4$ which gives the information related to changes in structure and composition. The peak observed 691 cm^{-1} (A_{1g}) vibration corresponds to Oh oxygen ions in Co 3p present in Co_3O_4 , and other two peaks were located at 484 cm^{-1} and 523 cm^{-1} combined vibration of Td and Oh oxygen atoms in the lattice. The observed three peaks were more sensitive to Ni 2p ion substituted in Co_3O_4 spinel lattice. Hence, the peak at 691 cm^{-1} come to be weak and shifted to lower frequencies, when Ni 2p exchanged in Co 3p in the Oh sites [39]. From the above vibrational peaks confirms the formation of $NiCo_2O_4$ because the peak were observed at 660, 503, 460 and 187 cm^{-1} corresponding to A_{1g} , F_{2g} , E_g , F_{2g} and modes of $NiCo_2O_4$ [40,41]. **Figure S1B** shows FT-IR studies of $NiCo_2O_4$. The peaks were observed at 555, 642 cm^{-1} correspond to M-O vibration of $NiCo_2O_4$. The peak at 1366 cm^{-1} may be associated with physically adsorbed CO_2 . The peaks at 1636 and 3484 cm^{-1} corresponding to vibration mode of absorbed water molecules [42].

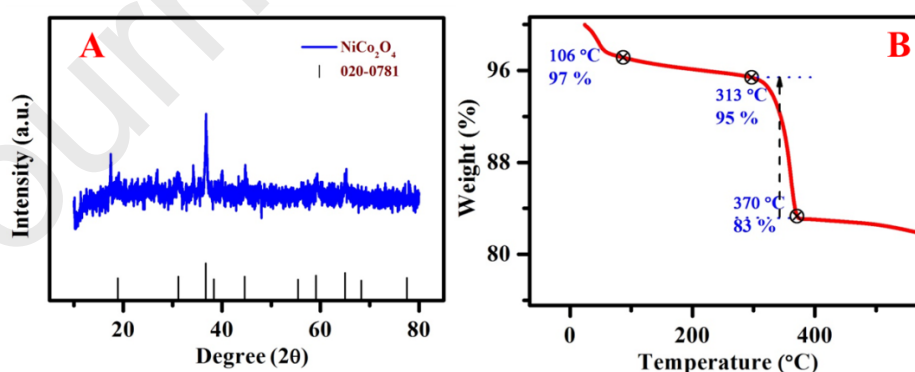


Figure 1 (A) XRD and (B) TGA of $NiCo_2O_4$ NR.

3.2 Morphological studies

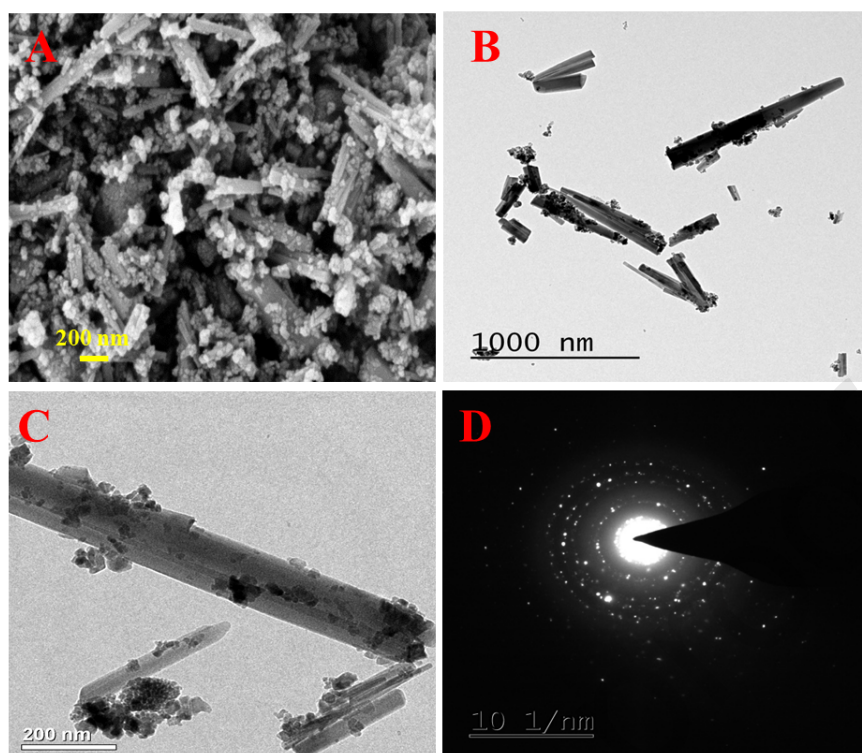


Figure 2 (A) FESEM; (B) TEM; (C) HRTEM images and (D) SAED pattern of NiCo_2O_4 NR.

The FESEM, TEM and HRTEM analysis were used as a tool to study the surface morphology, size of the nanostructure and SAED pattern of NiCo_2O_4 NR. **Figure 2A** gives the low magnification (FESEM) micrographs of the NiCo_2O_4 NR which shows that the as-synthesized material has broken nanorod as nanoparticle were situated on nanorod like structure. The TEM micrograph of the material was shown in **Figure 2B** where the NiCo_2O_4 NR micrograph was seen clearly. The observed morphological study, confirmed that the broken NR were situated on the NR. HRTEM morphology of NiCo_2O_4 NR was displayed in **Figure 2C**. **Figure 2D** displays a selected area electron diffraction (SAED) pattern of NiCo_2O_4 NR which clearly indicates that the NiCo_2O_4 NR was formed. The overall HRTEM and SAED results have clearly exposed the information about morphological, size and structure of the material.

Elemental mapping of NiCo_2O_4 NR is shown in **Figure 3A-D**. HRTEM micrograph of NiCo_2O_4 NR is shown in **Figure 3A** and insert of **Figure 3A** shows elemental mapping of all the three elements such as Ni, Co and O. **Figure 3 (B-D)** clearly display the elemental mapping of Ni, Co and O, respectively. These figures evidently confirm the formation of NiCo_2O_4 NR with well distribution of all three elements. The EDAX analysis also carried out using SEM techniques the result is shown in **Figure S2**. EDAX study also confirms the presence of Ni, Co and O elements without any other impurities.

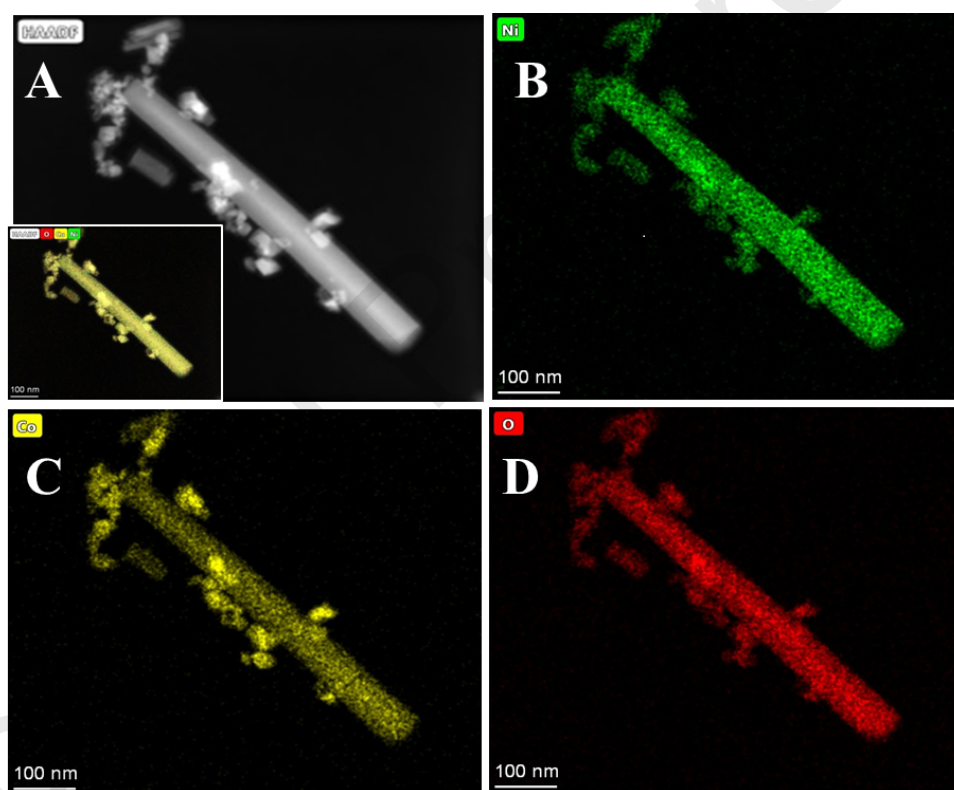


Figure 3 (A) HRTEM image; Elemental mapping of Ni (B), Co (C) and O (D) of NiCo_2O_4 NR.

3.3 X-ray photoelectron spectroscopic studies

The chemical composition, surface oxidation state and nature of the each component exist in the NiCo_2O_4 NR was analysed by XPS study. **Figure 4A** depicts the XPS survey spectrum of NiCo_2O_4 NR. Survey spectrum clearly identified the existence of Ni, Co and O without other impurities. Gaussian fitting method was used for the high magnification XPS studies of Co 2p, Ni 2p and O 1s spectrum which were shown in **Figures 4B-D**. **Figure 4B** shows that the fitted Ni 2p has two spin orbit doublets (Ni 2p_{3/2} and Ni 2p_{1/2} electronic configuration) two kind of Ni species has been found which are assigned to Ni²⁺ and Ni³⁺. Particularly, the peaks at the binding energies of 857.1 eV and 874.7 eV are characteristic of Ni³⁺ and the peaks observed at 855.3 eV and 872.9 eV correspond to Ni²⁺ [43].

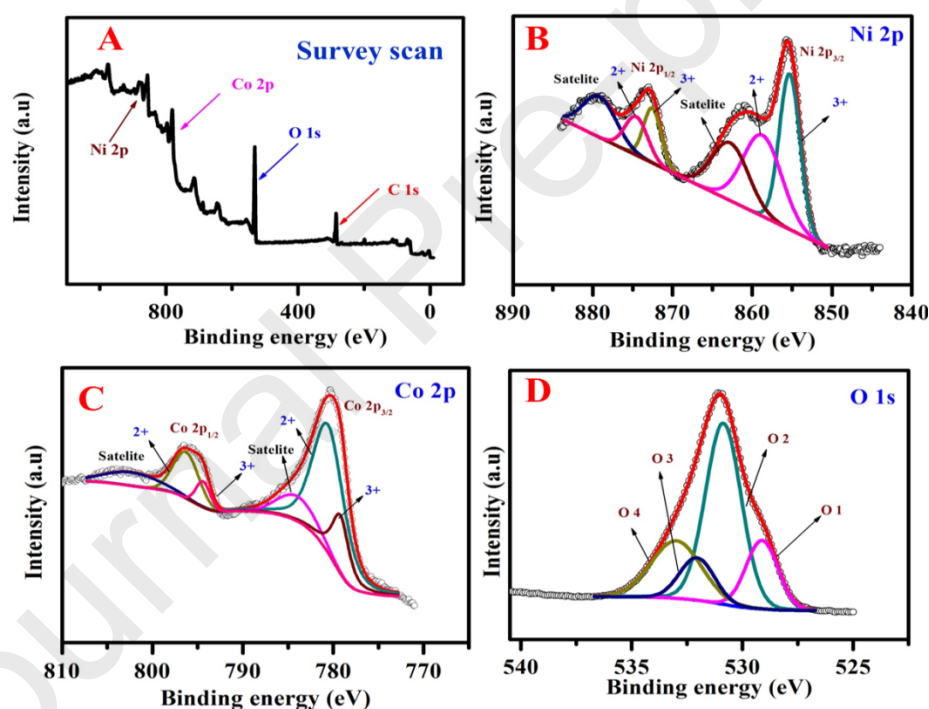


Figure 4 XPS study of NiCo_2O_4 NR (A) survey scan; (B) Ni 2p; (C) Co 2p and (D) O 1s.

The fitted Co 2p spectrum was displayed in **Figure 4C**. The Co 2p has two spin orbit doublets Co 2p_{3/2} and Co 2p_{1/2} electronic configuration at the binding energies of 779.4 eV and 794.3 eV corresponding to characteristic of Co²⁺ and Co³⁺, respectively. In this spectrum two shakeup satellite peaks (identified as “satellite”) were observed along with the two spin

orbit doublets [44]. The high resolution O 1s showed in **Figure 4D** exhibits four peaks at 529.3 eV (denoted as “O 1”), 530.7 eV (denoted as “O 2”), 531.8 eV (denoted as “O 3”) and 532.6 eV (denoted as “O 4”) was consigned to lattice oxygen in NiCo₂O₄ NR, oxygen in –OH, the defect sites with low oxygen coordination and chemisorbed/physisorbed water molecule on the surface respectively [43].

4. Electrochemical studies

4.1 Cyclic voltammetry comparison study

Cyclic voltammetric (CV) study was performed to assess the electrocatalytic behaviour of NiO/GCE, Co₃O₄/GCE and NiCo₂O₄ NR/GCE towards electro-oxidation of hydrazine as shown in **Figure S3**. This figure clearly displays that the NiCo₂O₄ NR demonstrates higher catalytic activity compared with NiO and Co₃O₄. **Figure 5** illustrates the CV of bare GCE and NiCo₂O₄ NR/GCE in the absence of hydrazine (curve ‘a’ and ‘b’) and the NiCo₂O₄ NR/GCE in the presence of 3 mM of hydrazine (curve ‘c’) in 0.1 M supporting electrolyte at a scan rate of 25 mV s⁻¹. The modified electrode shows abrupt increase in oxidation peak current value at much lower potential due to excellent electrocatalytic activity and high conductive nature of NiCo₂O₄ NR [16]. These observations intensely spotlight and indicate the electrocatalytic behaviour of modified electrode for hydrazine oxidation.

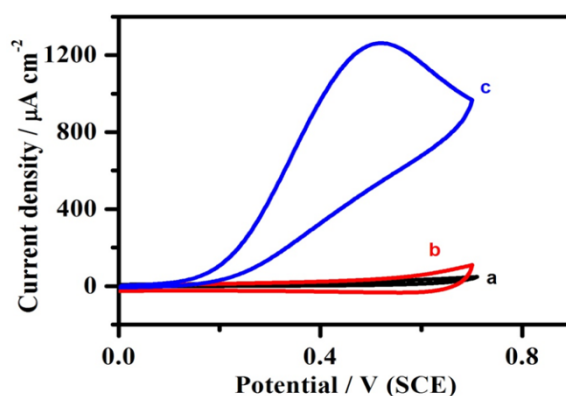


Figure 5 CV of bare GCE (a); NiCo₂O₄ NR/GCE in the absence of hydrazine (b) and NiCo₂O₄ NR/GCE in the presence of 3 mM hydrazine (c) at 25 mV s⁻¹.

4.2 pH effect

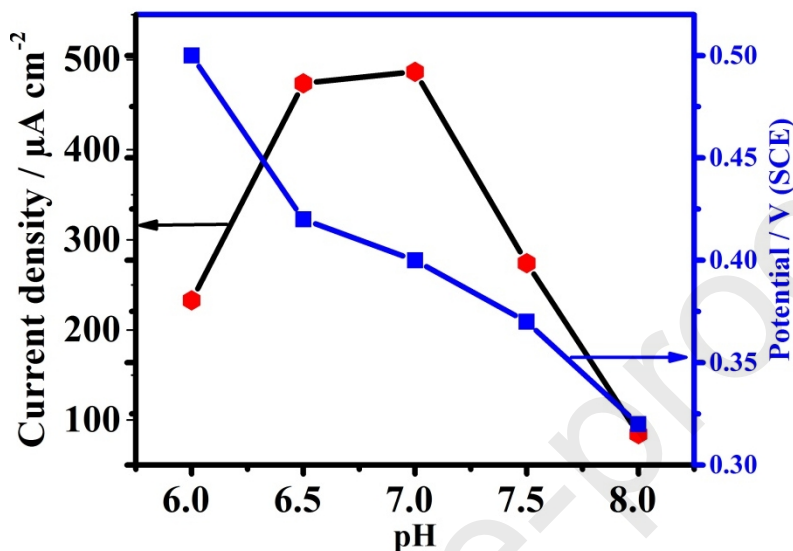


Figure 6 Effect of pH on peak current and peak potential for the electrooxidation of 2 mM of hydrazine at NiCo₂O₄ NR/GCE

Electrochemical oxidation of hydrazine depends on the solution pH. Due to this factor, optimisation of pH is essential for the efficient electrocatalytic detection of hydrazine.

Figure 6 shows as the pH of solution increases from 6.0, the peak current increases and peak potential shifts towards negative direction. The maximum peak current was observed at pH=7. Hence, pH 7 was chosen as optimum pH in the present study for the detection of hydrazine.

4.3 Effect of scan rate

In order to get the information on kinetics of electrochemical oxidation of hydrazine oxidation on NiCo₂O₄ NR/GCE, CV measurements were performed in 0.1 M PBS containing 3 mM of hydrazine at different scan rates as shown in **Figure S4A**. As shown in **Figure S4B**,

the anodic oxidation current increased linearly with square root of scan rate. Also, the slope of $\log(\text{peak current})$ vs $\log(\text{scan rate})$ plot (**Figure S4C**) was found to be nearly 0.5. These results explicitly show that the electrooxidation of hydrazine was controlled by the diffusion of electroactive species (i.e., hydrazine) from bulk to the electrode/electrolyte interface and the rate of electron transfer between the modified electrode and hydrazine is fast [45].

4.4 Effect of concentration

Figure 7A displays the catalytic performance of NiCo_2O_4 NR/GCE in various concentration of hydrazine. The oxidation peak was observed at 0.36 V and the oxidation peak current value also increased linearly with increase in the concentration of hydrazine from 0.07 to 6.0 mM. The corresponding current density vs. concentration plot is shown in **Figure 7B**. From the calibration plot, the linear range and sensitivity with correlation coefficient $R^2=0.998$ were found to be 0.07 to 1.78 mM, $290 \mu\text{A cm}^{-2} \text{mM}^{-1}$, respectively. The DPV of NiCo_2O_4 NR/GCE is shown in **Figure 7C** which showed that the anodic oxidation of hydrazine was observed at 0.25 V with respect to NiCo_2O_4 NR/GCE. Increasing the concentration of hydrazine the oxidation current value increases correspondingly. **Figure 7D** shows a plot of current density vs. the hydrazine concentration, which depicts linear correlation in the range of 0.01 to 2.25 mM. The best linear fitted equation $j_p (\mu\text{A}) = 48.25 \pm 1.6 (\text{mM}) + 2.56 \pm 1.8$ with a correlation coefficient $R^2 = 0.989$. The sensitivity and detection limit (LOD) were $48.25 \mu\text{A cm}^{-2} \text{mM}^{-1}$ and $0.26 \mu\text{M}$, respectively. Limit of qualification (LOQ) ($10 \times \text{standard deviation/slope}$) is $0.874 \mu\text{M}$. As shown in **Table 1**, the analytical factors such as sensitivity, linear range and detection limit concerning the sensing of hydrazine using NiCo_2O_4 NR/GCE which is compared with previous reports [46-54] based on various sensors. From the above table we can conclude that NiCo_2O_4 NR is a suitable catalyst for the hydrazine sensing.

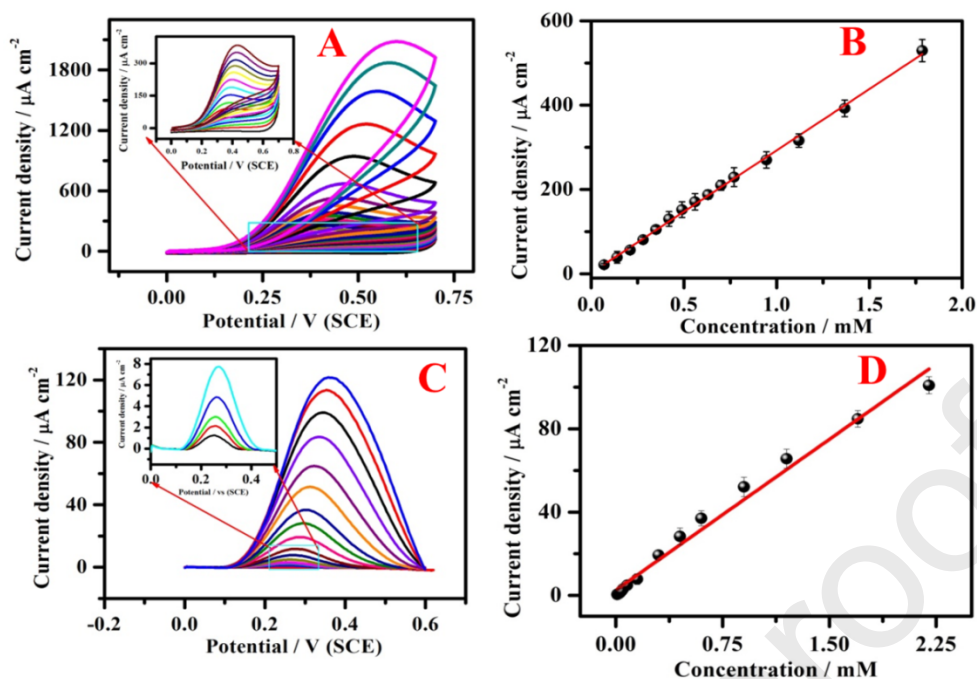


Figure 7 (A) CV response of NiCo₂O₄ NR/GCE in different concentration (0.07, 0.14, 0.21, 0.28, 0.35, 0.42, 0.49, 0.56, 0.63, 0.70, 0.77, 0.945, 1.12, 1.67, 1.78, 3.0, 4.0, 5.0 and 6.0 mM) of hydrazine; (B) A plot of j_{pa} vs. [hydrazine]; Scan rate at 5 mV s⁻¹; (C) DPV of NiCo₂O₄ NR modified electrode in hydrazine concentration range from 0.01 mM to 2.25 mM at the NiCo₂O₄ NR/GCE and (D) corresponding calibration curve.

Table 1 Comparison of the analytical performance of NiCo₂O₄ NR modified electrode with other sensors for the electrochemical hydrazine detection.

Sensor techniques	Linear range (μM)	Sensitivity	Limit of detection (μM)	Reference
Colorimetric sensor	6.0-40.0	-	1.1	[46]
	0.5-20.0	-	0.4	[47]
Chromatography	500-10000	-	20	[48]
	0.17-50	-	0.17	[49]

Fluorescence sensor	0.2-9.3	-	0.08	[50]
Electrochemical sensor	2.4-820	-	1.0	[51]
	0-1200	75 $\mu\text{A mM}^{-1}$	40	[52]
	0.07-500	-	0.04	[53]
	0.2-50	136.2 $\mu\text{A mM}^{-1}$ cm^{-2}	0.07	[54]
	3.0-300	-	1.0	[6]
	0.25-3400	270.0 $\mu\text{A mM}^{-1}$ cm^{-2}	0.06	[55]
	0.05-1600	1.95 $\mu\text{A mM}^{-1}$ cm^{-2}	0.028	[56]
	5.0-1300	449.7 $\mu\text{A mM}^{-1}$ cm^{-2}	1.4	[57]
	10-2250	48.25 $\mu\text{A mM}^{-1}$ cm^{-2}	0.26	Present work

As shown in **Table 1**, the analytical factors including sensitivity, linear range and limit of detection of NiCo_2O_4 NR/GCE are comparable with previous reports [46-54] based on various techniques. From the above table we can conclude that NiCo_2O_4 NR is a suitable catalyst for the electrochemical sensing of hydrazine.

4.5 Real sample analysis

In order to check the practical use of the proposed sensor (NiCo_2O_4 NR/GCE), hydrazine detection was carried out with different water samples. The as-collected water

samples from Karaikudi city, Tamil Nadu were tested for hydrazine concentration level in water without further pretreatment by proposed sensor technique. As collected water samples are found to be free from hydrazine (no peak response/signal) therefore, externally particular amount of hydrazine was spiked into the collected water samples to make the water contaminated. Following standard addition method the recoveries were examined by the catalytic current response corresponding results were displayed in **Table 2**. The observed results present reliable recovery with acceptable RSD values which indicates that our NiCo₂O₄ NR/GCE could be a potential candidate for the detection of hydrazine in practical purpose.

Table 2 Real sample analysis of hydrazine in real water samples by NiCo₂O₄ NR/GCE.

Samples	Detected	Added (μM)	Found[§] (μM)	Recovery (%)	RSD (%)
Sample 1	-	150	147	98.0	4.1
Sample 2	-	120	118	98.6	2.6

§-Standard addition method

4.6 Reproducibility and stability studies

Figure 8A shows the differential pulse voltammogram response recorded for the selectivity of hydrazine sensor and several common coexisting interfering substances (Cd²⁺, Pb²⁺, CaCl₂, NaNO₃, KCl, NaSO₄ and MgCl₂). The oxidation response was recorded for hydrazine and 20 times higher concentration of interferents. The outcome result depicts that no obvious current changes were observed for the interference. Hence, the interferents are not affecting the hydrazine oxidation. From this result we can conclude that our proposed sensor has excellent selectivity towards the detection of hydrazine. The stability of the sensor was

examined by cyclic voltammetry study. The NiCo₂O₄ NR shows good stability for the detection of hydrazine by retaining 89 % of the initial response after 50 cycles.

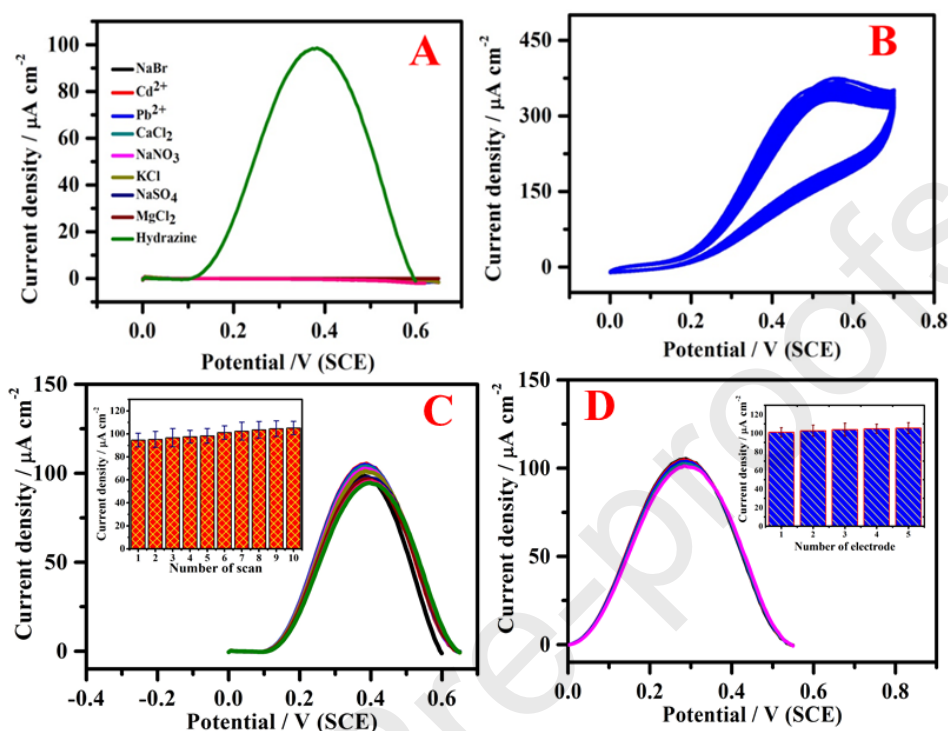


Figure 8 (A) Differential pulse voltammogram current response of NiCo₂O₄ NR for 0.02 M of hydrazine, 0.4 M of Cd²⁺, Pb²⁺, CaCl₂, NaNO₃, KCl, NaSO₄ and MgCl₂ interferences into 0.1 M PBS; (B) Cyclic voltammogram responses of the NiCo₂O₄ NR to 2 mM hydrazine in 0.1 M PBS (pH=7) for 50 cycles. Scan rate: 25 mV s⁻¹; (C) and (D) Differential pulse voltammogram of repeatability and fabrication reproducibility of NiCo₂O₄ NR modified electrode.

Reproducibility of the NiCo₂O₄ NR modified electrode for hydrazine determination was investigated using DPV. As shown in **Figure 8B**, the stability (50 cycles) of the modified electrode was examined in the presence of 2 mM of hydrazine at the scan rate of 25 mV s⁻¹. The relative standard deviation RSD was 4 %. Repeatability of the sensor was examined by repeating the measurement ten times with 5 mins interval of time and the results are displayed in **Figure 8C**. The peak current value and peak potential occurred at similar

position. The RSD value = 3.9 %. It indicates that our NiCo₂O₄ NR/GCE sensor has excellent repeatability for the electrooxidation of hydrazine. Finally, fabrication reproducibility (**Figure 8D**) (inter electrode) was examined by preparing five modified electrodes with same fabrication condition. All the electrodes gave excellent fabrication reproducibility with the RSD value of 1.6 %. From the above results we can conclude that our fabricated sensor has excellent reproducibility, stability, repeatability and selectivity.

5. Conclusion

In conclusion, NiCo₂O₄ NR has been synthesized by a simple hydrothermal approach. It has been characterized by several physiochemical and electrochemical techniques. XPS study confirms the formation of NiCo₂O₄ NR and the oxidation state of the material. The HRTEM study reveals that our synthesized material was NR like structure. In view of their unique structural advantage and electrochemical performance, the possibility of employing NiCo₂O₄ NR for the detection of hydrazine was carefully investigated. NiCo₂O₄ NR shows efficient catalytic performance for the detection of hydrazine with wide linear range and low limit of detection. The NiCo₂O₄ NR shows higher electrocatalytic activity for the detection of hydrazine oxidation compared with bare electrode. The proposed sensor depicts good sensitivity (48.25 $\mu\text{A cm}^{-2} \text{mM}^{-1}$), low LOD (260 nm), stability, reproducibility and selectivity. As-synthesised NiCo₂O₄ NR was used as a modified electrode in the field of analytical uses for the sensing of hydrazine in the analysed water samples. Hence, this work provides simple and efficient method for the sensing of hydrazine.

Acknowledgment

We thank the CSIR and UGC, New Delhi for the award of a UGC-Senior Research Fellowship for Mrs.V. Sudha. We wish to acknowledge the Central Instrumentation Facility (CIF), CSIR-CECRI, Karaikudi for characterization studies.

References

- [1] S.K. Mehta, K. Singh, A. Umar, G.R. Chaudhary, S. Singh, *Electrochim. Acta* 69 (2012) 128–133.
- [2] Y.J. Yang, W. Li, X. Wu, *Electrochim. Acta* 123 (2014) 260–267.
- [3] R. Madhu, B. Dinesh, S.M. Chen, R. Saraswathi, V. Mani, *RSC Adv.* 5 (2015) 54379–54386.
- [4] Y.Y. Tang, C.L. Kao, P.Y. Chen, *Anal. Chim. Acta* 711 (2012) 32–39.
- [5] P. Muthukumar, S.A. John, *J. Solid State Electrochem.* 18 (2014) 2393–2400.
- [6] C. Wang, L. Zhang, Z. Guo, J. Xu, H. Wang, K. Zhai, X. Zhuo, *Microchim. Acta* 169 (2010) 1–6.
- [7] E. Vernet, *Fundam. Appl. Toxicol.* 5 (1985) 1050–1064.
- [8] J.W. Mo, B. Ogorevc, X. Zhang, B. Pihlar, *Electroanalysis* 12 (2000) 48–54.
- [9] S. Amlathe, V.K. Gupta, *Analyst* 113 (1988) 1481–1483.
- [10] K. Ravichandran, R.P. Baldwin, *Anal. Chem.* 55 (1983) 1782–1786.
- [11] A. Ensafi, *Talanta* 47 (1998) 645–649.
- [12] Y.Y. Liu, I. Schmeltz, D. Hoffmann, *Anal. Chem.* 46 (1974) 885–889.
- [13] M. Michlmayr, D.T. Sawyer, *J. Electroanal. Chem. Interfacial Electrochem.* 23 (1969) 375–385.
- [14] C. Karuppiah, M. Velmurugan, S.-M. Chen, R. Devasenathipathy, R. Karthik, S.-F. Wang, *Electroanalysis* 28 (2016) 808–816.

- [15] R. Devasenathipathy, V. Mani, S.-M. Chen, *Talanta* 124 (2014) 43–51.
- [16] C. Yuan, H. Bin Wu, Y. Xie, X.W.D. Lou, *Angew. Chemie Int. Ed.* 53 (2014) 1488–1504.
- [17] S. and Y.N. O. Knop, K. I. G. Reid, *Can. J. Chem.* 46 (1968) 3463–3476.
- [18] P.D. Battle, A.K. Cheetham, J.B. Goodenough, *Mater. Res. Bull.* 14 (1979) 1013–1024.
- [19] B. Kaur, B. Satpati, R. Srivastava, *New J. Chem.* 39 (2015) 1115–1124.
- [20] X.Y. Yu, X.Z. Yao, T. Luo, Y. Jia, J.H. Liu, X.J. Huang, *ACS Appl. Mater. Interfaces* 6 (2014) 3689–3695.
- [21] W. Huang, Y. Cao, Y. Chen, J. Peng, X. Lai, J. Tu, *Appl. Surf. Sci.* 396 (2017) 804–811.
- [22] S. Liu, J. Wu, J. Zhou, G. Fang, S. Liang, *Electrochim. Acta* 176 (2015) 1–9.
- [23] T.H. Ko, K. Devarayan, M.K. Seo, H.Y. Kim, B.S. Kim, *Sci. Rep.* 6 (2016) 1–9.
- [24] J. Li, S. Xiong, Y. Liu, Z. Ju, Y. Qian, *ACS Appl. Mater. Interfaces* 5 (2013) 981–988.
- [25] L. Qian, L. Gu, L. Yang, H. Yuan, D. Xiao, *Nanoscale* 5 (2013) 7388–7396.
- [26] G. Zhang, X.W.D. Lou, *Sci. Rep.* 3 (2013) 2–7.
- [27] L. Yu, G. Zhang, C. Yuan, X.W. Lou, *Chem. Commun.* 49 (2013) 137–139.
- [28] G.Q. Zhang, H. Bin Wu, H.E. Hoster, M.B. Chan-Park, X.W. Lou, *Energy Environ. Sci.* 5 (2012) 9453–9456.
- [29] G. Zhang, X.W.D. Lou, *Adv. Mater.* 25 (2013) 976–979.

- [30] M.U. Anu Prathap, R. Srivastava, *Electrochim. Acta* 108 (2013) 145–152.
- [31] T.-H. Ko, K. Devarayan, M.-K. Seo, H.-Y. Kim, B.-S. Kim, *Sci. Rep.* 6 (2016) 20313.
- [32] Y. Mo, Q. Ru, J. Chen, X. Song, L. Guo, S. Hu, S. Peng, *J. Mater. Chem. A* 3 (2015) 19765–19773.
- [33] J. Wu, R. Mi, S. Li, P. Guo, J. Mei, H. Liu, W.M. Lau, L.M. Liu, *RSC Adv.* 5 (2015) 25304–25311.
- [34] W. Zhou, D. Kong, X. Jia, C. Ding, C. Cheng, G. Wen, *J. Mater. Chem. A* 2 (2014) 6310–6315.
- [35] X. Liu, S. Shi, Q. Xiong, L. Li, Y. Zhang, H. Tang, C. Gu, X. Wang, J. Tu, *ACS Appl. Mater. Interfaces* 5 (2013) 8790–8795.
- [36] Y. Lei, J. Li, Y. Wang, L. Gu, Y. Chang, H. Yuan, D. Xiao, *ACS Appl. Mater. Interfaces* 6 (2014) 1773–1780.
- [37] G.-Y. Zhang, B. Guo, J. Chen, *Sensors Actuators B Chem.* 114 (2006) 402–409.
- [38] M. Kundu, G. Karunakaran, E. Kolesnikov, V.E. Sergeevna, S. Kumari, M. V. Gorshenkov, D. Kuznetsov, *J. Ind. Eng. Chem.* 59 (2018) 90–98.
- [39] C.F. Windisch, G.J. Exarhos, R.R. Owings, *V J. Appl. Phys.* 95 (2004) 5435–5442.
- [40] W. Xiong, Y. Gao, X. Wu, X. Hu, D. Lan, Y. Chen, X. Pu, Y. Zeng, J. Su, Z. Zhu, *ACS Appl. Mater. Interfaces.* 6 (2014) 19416–19423.
- [41] E. Umeshbabu, G. Rajeshkhanna, P. Justin, G.R. Rao, *Mater. Chem. Phys.* 165 (2015) 235–244.
- [42] G. Karunakaran, M. Jagathambal, M. Venkatesh, G. Suresh Kumar, E. Kolesnikov, A.

- Dmitry, A. Gusev, D. Kuznetsov, Powder Technol. 305 (2017) 488–494.
- [43] C. Yuan, J. Li, L. Hou, X. Zhang, L. Shen, X.W.D. Lou, Adv. Funct. Mater. 22 (2012) 4592–4597.
- [44] B. Cui, H. Lin, Y. Liu, J. Li, P. Sun, X. Zhao, C. Liu, J. Phys. Chem. C. 113 (2009) 14083–14087.
- [45] J. Wu, T. Zhou, Q. Wang, A. Umar, Sensors Actuators B Chem. 224 (2016) 878–884.
- [46] B. Zargar, A. Hatamie, Sensors Actuators B Chem. 182 (2013) 706–710.
- [47] Y. He, W. Huang, Y. Liang, H. Yu, Sensors Actuators B Chem. 220 (2015) 927–931.
- [48] G. Elias, W.F. Bauer, J. Sep. Sci. 29 (2006) 460–464.
- [49] J. Zhang, L. Ning, J. Liu, J. Wang, B. Yu, X. Liu, X. Yao, Z. Zhang, H. Zhang, Anal. Chem. 87 (2015) 9101–9107.
- [50] X. Chen, Y. Xiang, Z. Li, A. Tong, Anal. Chim. Acta 625 (2008) 41–46.
- [51] S.J.R. Prabakar, S.S. Narayanan, J. Electroanal. Chem. 617 (2008) 111–120.
- [52] K.K. Lee, P.Y. Loh, C.H. Sow, W.S. Chin, Biosens. Bioelectron. 39 (2013) 255–260.
- [53] H. Beitollahi, S. Tajik, S. Jahani, Electroanalysis 28 (2016) 1093–1099.
- [54] X. Gu, X. Li, S. Wu, J. Shi, G. Jiang, G. Jiang, S. Tian, RSC Adv. 6 (2016) 8070–8078.
- [55] Y. Dong, Z. Yang, Q. Sheng, J. Zheng, Colloids Surfaces A Physicochem. Eng. Asp. 538 (2018) 371–377.
- [56] S. Sakthinathan, S. Kubendhiran, S.M. Chen, P. Sireesha, C. Karupppiah, C. Su,

Electroanalysis 29 (2017) 587–594.

- [57] Z. Yang, Q. Sheng, S. Zhang, X. Zheng, J. Zheng, *Microchim. Acta* 184 (2017) 2219–2226.

Journal Pre-proofs